Assessing Uncertainty and Repeatability in Time-lapse VSP Monitoring of CO_2 Injection in a Brine Aquifer, Frio Formation, Texas (A case study)

Siamak Nazari[1] and Thomas M. Daley[2]

[1]University of California, Berkeley, Department of Civil and Environmental Engineering Berkeley, CA 94720

[2]Earth Sciences Division, Lawrence Berkeley National Lab, 1 Cyclotron Road Berkeley, CA 94720

NRAP-TRS-III-00X-2013

Level III Technical Report Series

07 February 2013

This page intentionally left blank

Table of Contents

List of Figures

List of Tables

Acronyms and Abbreviations

Term	Description
VSP	Vertical Seismic Profile
NRMS	Normalized Root Mean Squared

Acknowledgments

This work was completed as part of the National Risk Assessment Partnership's (NRAP) effort to understand the risk of wells and well borings regarding leakage of CO_2 and brine in response to geologic carbon storage, Support for this project came from the Crosscutting Research program, through the Assistant Secretary for Fossil Energy, Office of Sequestration, Hydrogen, and Clean Coal Fuels, of the U.S. Department of Energy, under Contract No. DE-AC02-05CH11231. The authors wish to acknowledge Robert Romanosky (NETL Strategic Center for Coal) and Regis Conrad (DOE Office of Fossil Energy) for programmatic guidance, direction, and support.

This work was performed as a Masters degree project with guidance from Prof. J. Rector of the Univ. of California, Berkeley.

The authors would like to thank Dr. Susan Hovorka of the Bureau of Economic Geology, the Gulf Coast Carbon Center and the Univ. of Texas, Austin, for her guidance and support of the Frio project and the VSP work. We would also like to thank the reviewers of this report.

1. ABSTRACT

This study was done to assess the repeatability and uncertainty of time-lapse VSP response to CO_2 injection in the Frio formation near Houston Texas. A work flow was built to assess the effect of time-lapse injected CO_2 into two Frio brine reservoir intervals, the 'C' sand (Frio1) and the 'Blue sand' (Frio2). The time-lapse seismic amplitude variations with sensor depth for both reservoirs Frio1 and Frio2 were computed by subtracting the seismic response of the base survey from each of the two monitor seismic surveys. Source site 1 has been considered as one of the best sites for evaluating the time-lapse response after injection. For site 1, the computed time-lapse NRMS levels after processing had been compared to the estimated time-lapse NRMS level before processing for different control reflectors, and for brine aquifers Frio1, and Frio2 to quantify detectability of amplitude difference.

As the main interest is to analyze the time-lapse amplitude variations, different scenarios have been considered. Three different survey scenarios were considered: the base survey which was performed before injection, monitor1 performed after the first injection operation, and monitor2 which was after the second injection. The first scenario was base-monitor1, the second was base-monitor2, and the third was monitor1-monitor2. We considered three 'control' reflections above the Frio to assist removal of overburden changes, and concluded that third control reflector (CR3) is the most favorable for the first scenario in terms of NRMS response, and first control reflector (CR1) is the most favorable for the second and third scenarios in terms of NRMS response. The NRMS parameter is shown to be a useful measure to assess the effect of processing on time-lapse data. The overall NRMS for the Frio VSP data set was found to be in the range of 30% to 80% following basic processing. This could be considered as an estimated baseline in assessing the utility of VSP for CO_2 monitoring.

This study shows that the CO_2 injection in brine reservoir Frio1 (the 'C' sand unit) does induce a relative change in amplitude response, and for Frio2 (the 'Blue' sand unit) an amplitude change has been also detected, but in both cases the uncertainty, as measured by NRMS indicates the reservoir changes are, at best, only slightly above the noise level, and often below the noise level of the overall data set.

2. INTRODUCTION

Time-lapse seismic is series of repeated reflection seismic surveys over the same location and serves, among other uses, as a constraint to reservoir simulation models for identifying fluid flow. This kind of survey has become a widely used method for monitoring reservoir fluid behavior during production and development stages of a reservoir.

Although 3D seismic imaging, using surface sources and receivers, has been the primary tool used for geophysical reservoir monitoring to date, vertical seismic profiling (VSP) has characteristics that make this technique particularly suitable for time-lapse surveying. In particular, the use of downhole receivers provides some potential advantages: (1) Increased frequency content improves vertical and lateral resolution, allowing the examination of the reservoir in greater detail, both statically and dynamically. (2) Improved signal-to-noise ratio permitting the measurement and quantification of time-lapse changes in the reservoir with a higher degree of confidence.

The objectives of this work are to 1) analyze the two Frio VSPs in a consistent manner for the detection of CO_2 induced changes in seismic reflectivity and 2) quantify the uncertainty in the VSP data which controls the quantitative interpretation of the time-lapse change. To quantify time-lapse uncertainty, we use the normalized root mean square (NRMS) method of Kragh and Christie (2002). NRMS is a measure of data similarity, expressed as a percentage (from 0 to 200) with lower values having greater similarity. NRMS will be defined and discussed in Section 6.

3. TIME-LAPSE VSP MONITORING – ASSESSING RISK

The motivation for VSP can be demonstrated using a methodology developed by Lumley (1997) as a "risk analysis spreadsheet." An enhanced version of the spreadsheet has been developed for both time lapse VSP and 4D seismic reservoir monitoring projects by Lumley et al. (2000). In Figure 1, the significant new parameters developed for this study include measures of vertical and lateral resolution, source and receiver repeatability and image aperture area, relevant for both VSP and 3D seismic acquisition. A scoring system quantifies the risk measured in each new parameter for both type of methods. These parameters were quantified for six injection scenarios in different kind of reservoirs around the world (Figure 1A). The six scenarios include CO_2 injection in land-based carbonate reservoirs, steam injection in land-based sand reservoirs, and waterflood in marine-based sand reservoirs, all focused on monitoring a 7-meters thin target zone. The six scenarios are fully evaluated in terms of reservoir and seismic parameters, and cross-plotted in a final combined analysis of all parameters. The results show that VSP has the potential to be of much lower risk than 4D seismic for all six scenarios, provided that VSP surveys are highly repeatable, and attain excellent frequency content, areal coverage and image quality.

Table 1: List of reservoir and seismic parameters used, in spreadsheet (Lumley, 2000) for VSP versus 3D seismic time lapse risk analysis

RESERVOIR PARAMETERS	SEISMIC PARAMETERS
Porosity	Vertical resolution
Dry rock bulk modulus	Horizontal resolution
Fluid compressibility contrast	Source repeatability
Fluid saturation changes	Receiver repeatability
Predicted impedance changes	Survey repeatability
Structural dip	Image aperture area
	Image quality
	Imaging of fluid contacts

The spreadsheet that was presented by Lumley (2000) follows two goals:

(1) Quantifying the risk of doing time lapse VSP, and

(2) To compare the risk of VSP survey versus 4D seismic for a given monitoring objective.

Reservoir and seismic parameters for the VSP method have been categorized by a scoring system to attain an acceptable risk analysis in terms of the relationship between both set of parameters (Figure 1). Both reservoir and seismic parameters are assigned a score of 0-5 points depending on how they improve the chance of success of a reservoir monitoring project. According to Figure 1(A), favorable reservoir candidates for seismic monitoring have high porosity, low dry-rock bulk modulus (high compressibility), large fluid compressibility contrast between the fluids being monitored, large saturation change (reservoir sweep), large changes in predicted seismic impedance or travel time and low structural dip. A suitable technique for reservoir monitoring should have high vertical and horizontal resolution, excellent repeatability for source, receiver

and overall survey acquisition, large image aperture area, excellent image quality, and ability to image fluid contacts.

A

	Ideal		W. Texas vuggy carb. CO2		W. Texas gran. carb. CO2		San Joaquin sand steam		Indonesia sand steam		GoM/Nsea soft sand waterflood		GoM/Nsea med. Sand waterflood	
	3D	VSP	3D	VSP	3D	VSP	3D	VSP	3D	VSP	3D	VSP	3D	VSP
RESERVOIR PARAMETERS														
Porosity	5	5	3	3	1.5	1.5	4	4	5	5	4.5	4.5	3.5	3.5
Dry rock bulk modulus	5	5	2	2	1	1	3	3	5	5	4.5	4.5	3.5	3.5
Fluid compressibility contrast	5	5	5	5	5	5	5	5	5	5	4.5	4.5	3	3
Fluid saturation change	5	5	5	5	5	5	5	5	5	5	5	5	3.5	3.5
Predicted impedance change	5	5	2	2	1	1	5	5	5	5	5	5	4	4
Structural dip	5	5	5	5	5	5	4	4	5	5	3.5	3.5	3.5	3.5
RESERVOIR TOTAL %	100	100	73	73	62	62	87	87	100	100	90	90	70	70
SEISMIC PARAMETERS														
Vertical resolution	5	5	**0**	1	**0**	**0**	**0**	1.5	1.5	2.5	**0.5**	1.5	**0**	**0**
Horizontal resolution	5	5	**0**	1	**0**	**0**	**0**	2	1.5	2.5	**0.5**	1.5	**0**	**0**
Source repeatability	5	5	3	4	3	4	3	4	3	4	3	4	3	4
Receiver repeatability	5	5	3	5	3	5	3	5	3	5	2	5	2	5
Survey repeatability	5	5	4	5	4	5	4	5	4	5	3	5	3	5
Image aperture area	5	5	5	3	5	3	5	3	5	3	5	3	5	3
Image quality	5	5	2	4	2	4	2	4	2	4	2	4	2	4
Imaging of fluid contacts	5	5	2	4	2	4	2	4	2	4	2	4	2	4
SEISMIC TOTAL %	100	100	**48**	68	**48**	**63**	**48**	70	55	75	**45**	70	**43**	**63**

B

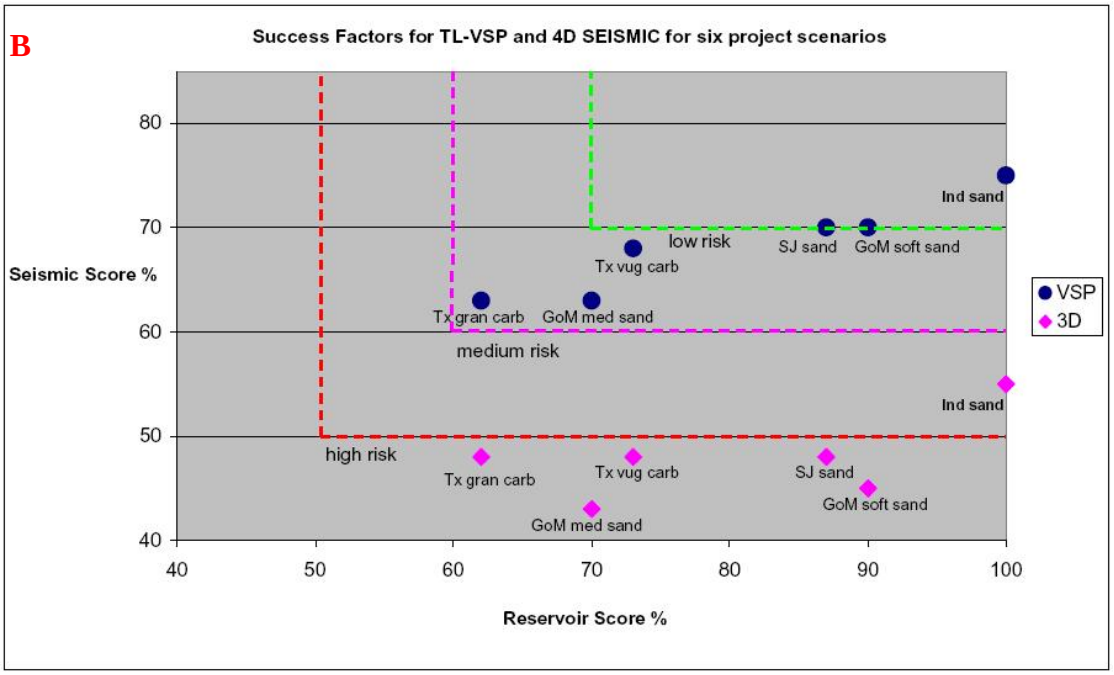

Figure 1: A risk analysis spreadsheet and chart for time-lapse VSP and 4D seismic, (A) scoring of reservoir and seismic parameters, (B) risk analysis of seismic scores versus reservoir scores for six projects (from Lumley, 2000).

Examining the seismic scores, in all cases the VSP score for each scenario exceeds the 3D seismic score. This is, in part, because the reservoir scenarios favor VSP by focusing on a thin 7-meters thick target zone; an important high-resolution reservoir target that 3D seismic is not very good at imaging but VSP is. The difference in scores is also partially due to the fact that VSP surveys tend to have much better receiver repeatability, somewhat better source and overall

survey repeatability, and the potential for better image quality. However, these aspects of image quality depend critically on whether the VSP data is recorded with high enough frequency content, fold and signal-to-noise ratio. In comparison, 3D seismic surveys tend to have a wider image aperture area and higher signal-to-noise ratio than VSP, but have lower resolution and acquisition repeatability. In general, the land surveys score better than the marine surveys. This is because seismic acquisition repeatability, both 3D and VSP, was traditionally more easily achieved on land than at sea (Lumley et al., 2000). [3] However, development of marine seismic technology (both location tracking and active control of streamers) has, in the last 10+ years, reversed this situation in most cases. For new, or very recent marine surveys, the expectation of repeatability is typically better than land surveys. Additionally, marine surveys are more likely to employ permanent of semi-permanent sensor arrays (located on the sea floor). Nonetheless, the comparison of surface and borehole surveys under the Lumley methodology is still valid.

Using the rule of thumb that a project scenario must score greater than 60% on its seismic parameters to proceed with a monitoring project, Lumley (2000) shows that none of the 3D seismic scenarios passes this test, whereas all of the VSP scenarios exceed this risk threshold. Finally, it is concluded that VSP projects can be more cost-effective than 3D seismic surveys. The total project risk is shown in the Table 2.

Table 2: Total project risk

	4D	VSP
Indonesia sand, steam injection	Med-High	Low
GoM-Nsea soft sand, high-GOR oil, waterflood	High	Med-low
San Joaquin sand, steam injection	High	Med-low
W. Texas vuggy carbonates, CO_2 injection	High	Med-low
GoM/Nsea medium sand, low-GOR oil, waterflood	High	Medium
W. Texas granular carbonates, CO_2 injection	High	Medium

4. FRIO VSP BACKGROUND

The Frio Brine Pilot was an early test geosequestration in a brine reservoir. The Frio pilot project is described in Hovorka, et al. 2006. There were two injections of CO_2 as part of the Frio project. These injections were in reservoirs intervals known as the C sand and the Blue sand, hereafter named "Frio1" and "Frio2," located in the Frio Formation, at depths ~5000ft and ~5400ft respectively near Houston, Texas. Injection into reservoir Frio1 was in 2004 and Frio2 injection was in 2009. Three VSP surveys were acquired, a pre and post injection for Frio-1 and a post injection for Frio-2. Acquisition and initial analysis of the Frio-1 VSP is described in Daley, et al, 2008, while initial results from the Frio-2 VSP were presented by Daley and Hovorka, 2011. Other studies based on the Frio Pilot are described in Hovorka, et al, 2006, Zhou, et al, 2010 and Daley, et al, 2011. The three VSP surveys all used the same sensor string (an 80-level 3-component borehole geophone array) and all used explosive sources located at the same location to the extent possible with shothole drilling in a forested area.

5. DATA PROCESSING

This study begins with data preprocessed to provide upgoing reflectivity sections, with consistent parameters to preserve amplitudes (SR2020, 2009). Figure 2 describes the general processing work-flow used in this study, with specific steps summarized here.

Data preparation and QC: raw VSP data sets were input into the processing software and checked to insure that the three data sets, hereafter called base, monitor1, and monitor2, have consistent geometry information in the trace headers. The software used for this purpose is called ECHOS, supported by Paradigm Ltd, which is developed for processing of seismic data.

Preprocessing of data: the three sets of data have been processed using the same parameters. The flow developed is shown in Figure 2 and includes data alignment, data flattening, median filtering, and static shift. The data flattening is done to align the upgoing reflections at a constant time by applying a shift equal to twice the first arrival time for each depth recording. The median filtering is done to smooth the trace-to-trace variations in the upgoing reflection. The static shift is applied to a control reflector to remove shallow velocity variations which are not due to the reservoir processes (CO_2 injection). These shallow variations include source variability and near-surface saturation changes.

Data Subtraction: three data sets have been subtracted from one another to get the difference section. Different control reflectors have been picked and compared and gathers have been flattened based on those control reflectors to enhance the signal to noise ratio and the level of NRMS.

Normalized RMS amplitude (NRMS) calculation: the normalized RMS amplitude level for subtracted base- monitor1, base-monitor2, and monitor1-monitor2 has been calculated to assess the improvement in time-lapse amplitude normalization before and after preprocessing.

Time-lapse amplitude interpretation: relative RMS amplitude levels have been computed and compared for several control reflectors, and the reflections from reservoir Frio1 and reservoir Frio2.

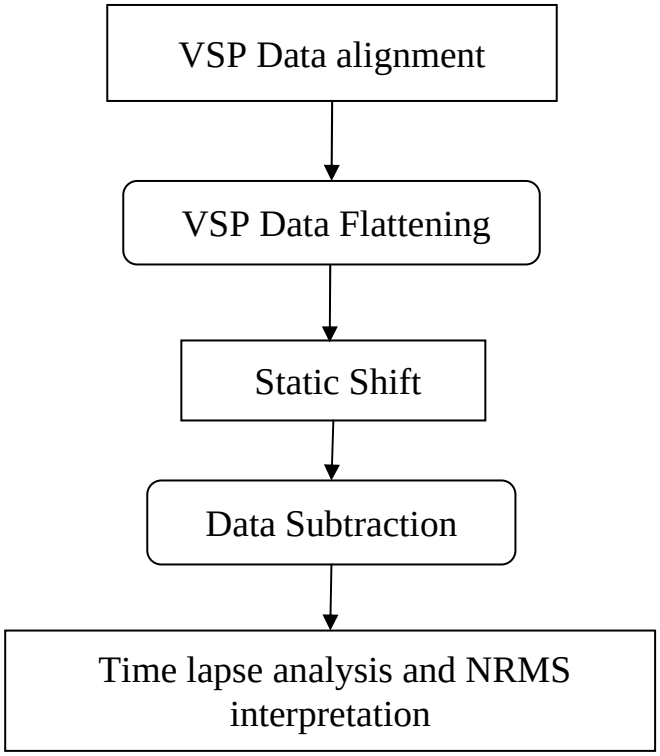

Figure 2: Schematic flow-chart of the time-lapse work-flow.

6. DATA PREPARATION AND PREPROCESSING

VSP data have been time-shifted for different source sites by adding the first break time to the trace header of the data. This aims to have all the reflected events horizontally aligned for better processing and interpretation.

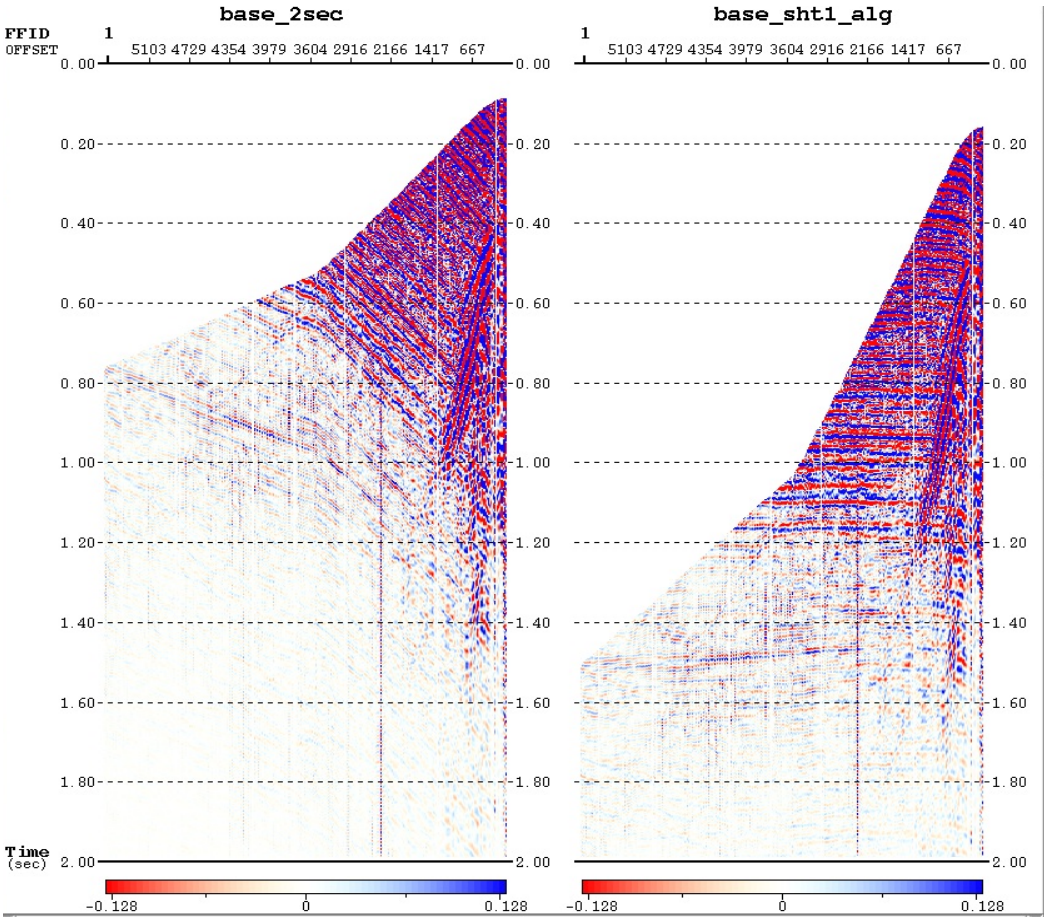

Figure 3: raw data (left) and aligned data for base survey (right) for site 1.

Figure 3 depicts the original upgoing 'raw' data and the aligned data for base survey of time-lapse study. The first break time has been added to the time trace header to apply a shift which leaves the reflected events horizontally aligned. Figure 4 and 5 also show the aligned data for monitor 1 and monitor 2 surveys.

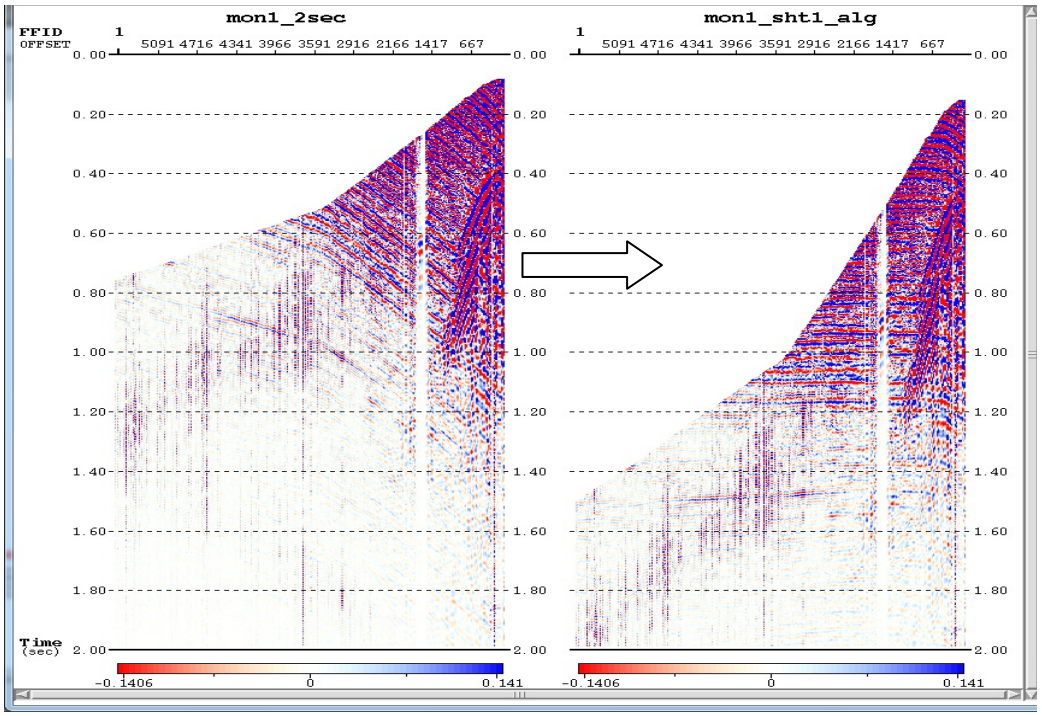

Figure 4: raw data (left) and aligned data for monitor1 survey (right) for site1.

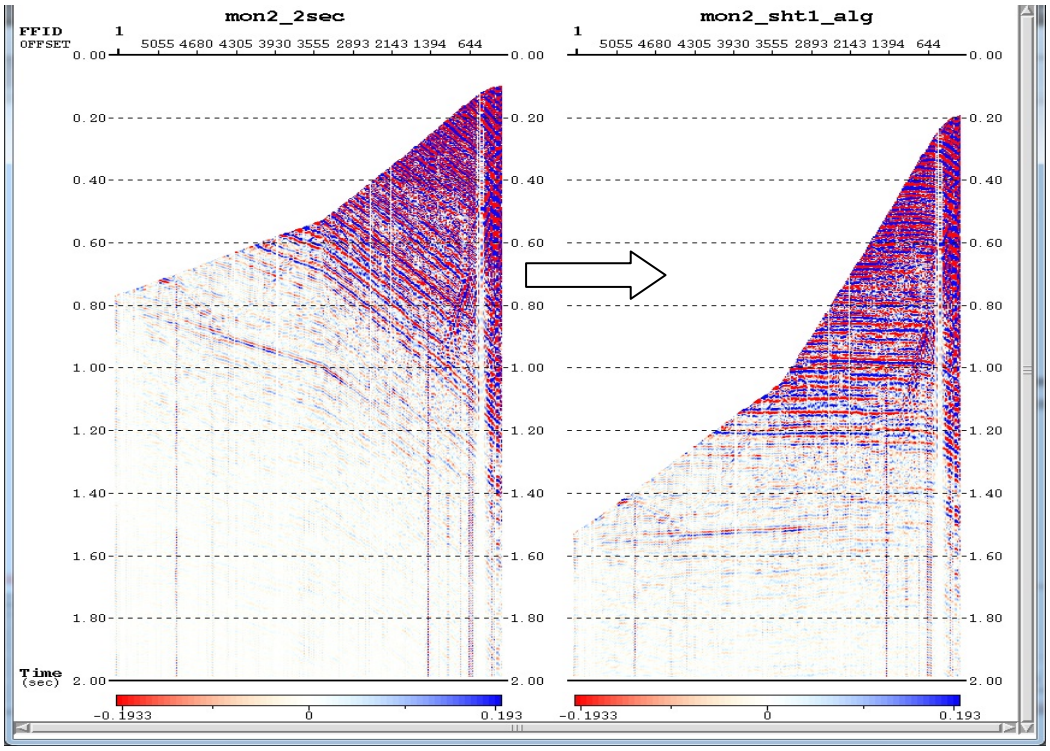

Figure 5: raw data (left) and aligned data for monitor2 survey (right) for site1.

The data smoothing (median) filter has been applied to all base and monitors data sets to enhance the spatial coherence of the control reflector for time picking.

The next step was picking a control reflector horizon to use for time shifting the three data sets. In this regards, different control reflectors have been picked and tested to improve the level of NRMS of the signal amplitude.

Figure 6 shows the smoothing (median filter) and flattening (time shift) processes for base survey at site1.

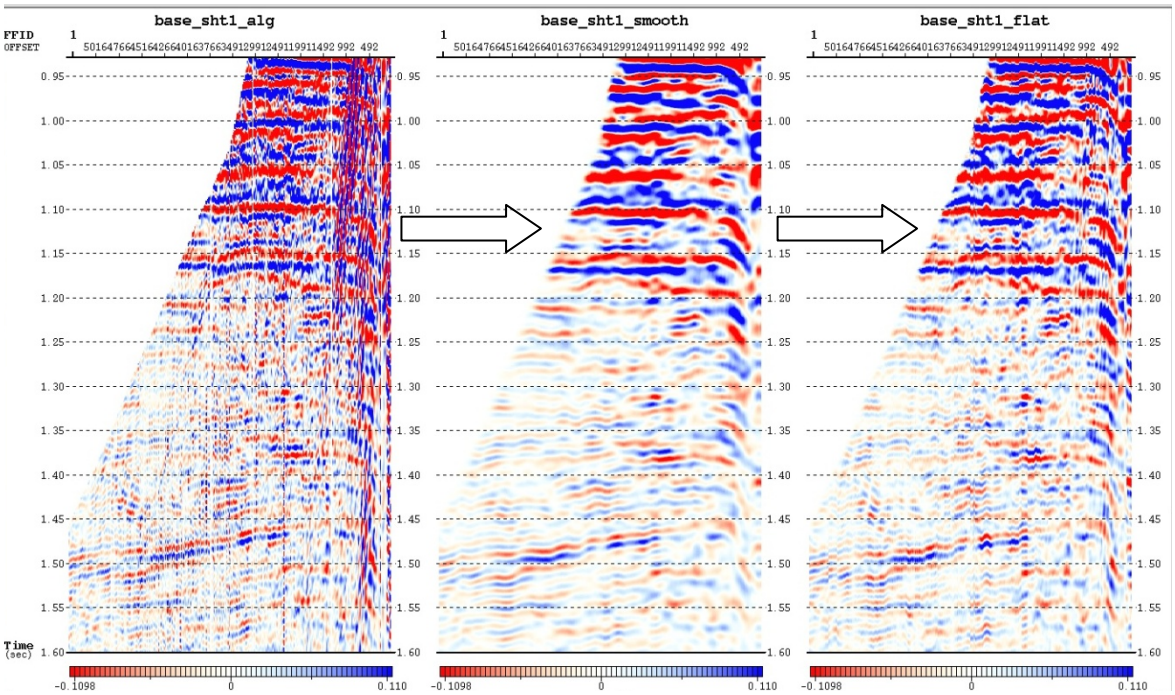

Figure 6: data smoothing (middle) and flattening (right) for base scenario for site1

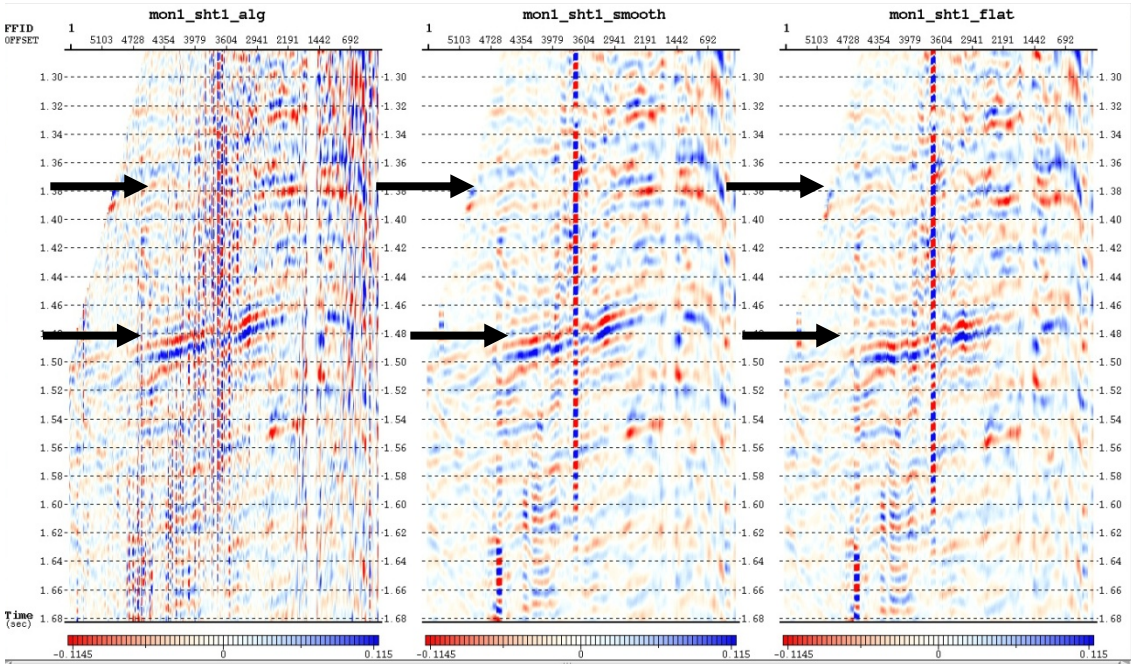

Figure 7: data smoothing/flattening for monitor1 (with arrows showing reservoirs 1and2, upper and lower) for source site1.

Figures 7 and 8 show the smoothing and flattening processing data for monitor1 and monitor 2 data.

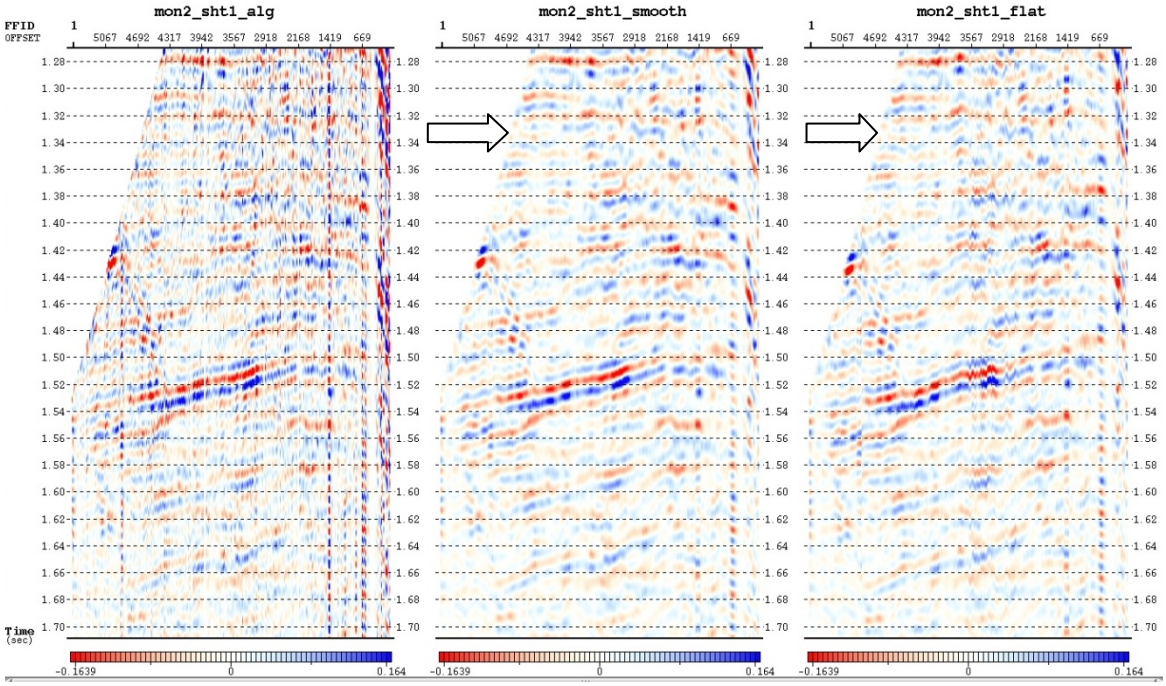

Figure 8: data smoothing and flattening for monitor2 scenario for site 1

Three data sets, base, monitor1, and monitor2, have been processed with the same parameters. The processing steps include median filter smoothing, flattening and then static time shift has been applied to monitor1 and monitor2 data sets to shift the control reflector for all three data sets to the same travel time. The time shift should result in more accurate time-lapse amplitude difference as both base and monitors should be aligned at the same level for subtraction.

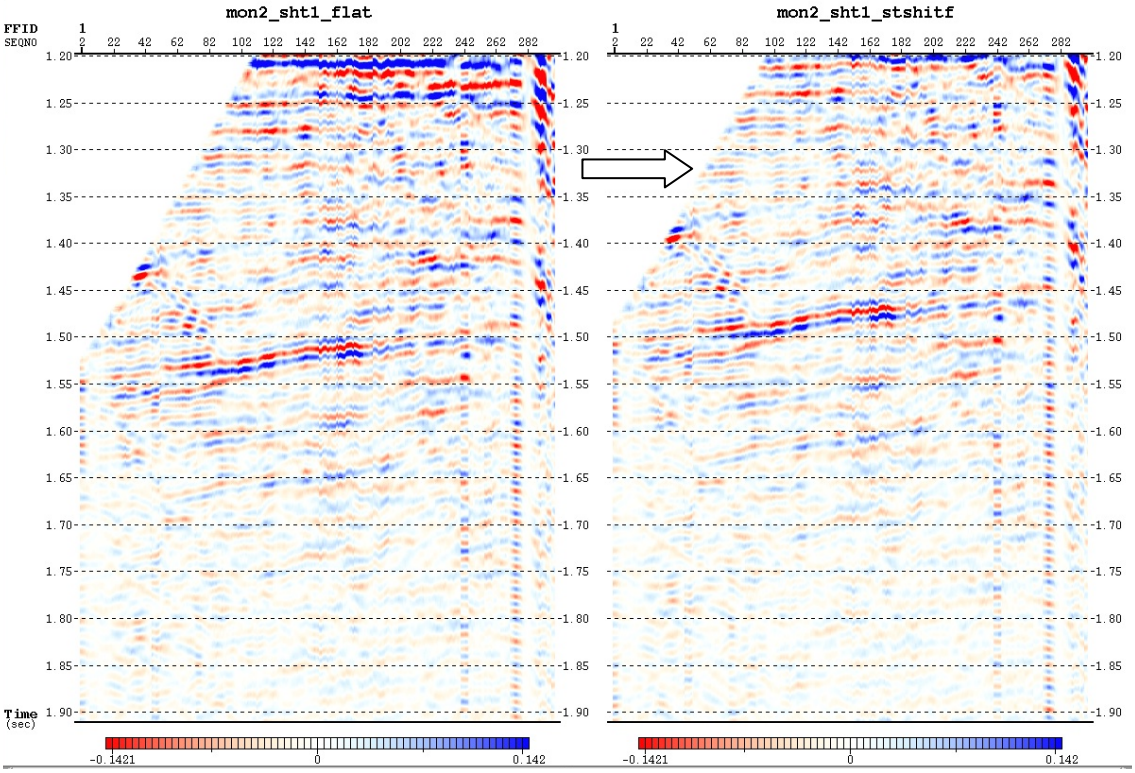

Figure 9: applying static time shift to the flattened data, monitor2 for site1

6.1 DATA SUBTRACTION

After applying static time shift to the monitor data sets, data differencing is done to enhance the effect of time-lapse amplitude response after CO_2 injection for each base-monitor1, base-monitor2, and monitor1-monitor2 scenario. An Echoes processing flow has been written for subtracting the data (Figure 10). Figure11 shows data that have been prepared and are ready for subtraction from one another.

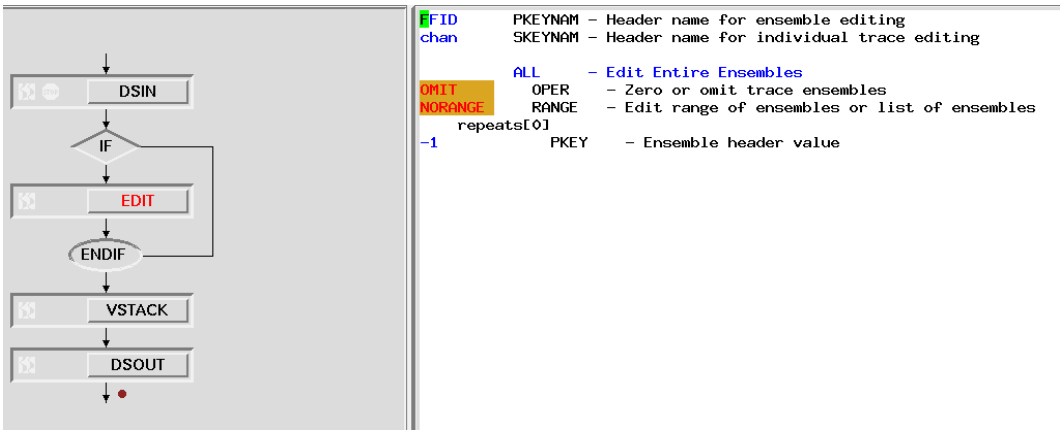

Figure 10: processing flow for subtracting base, monitor1, and monitor 2 data sets.

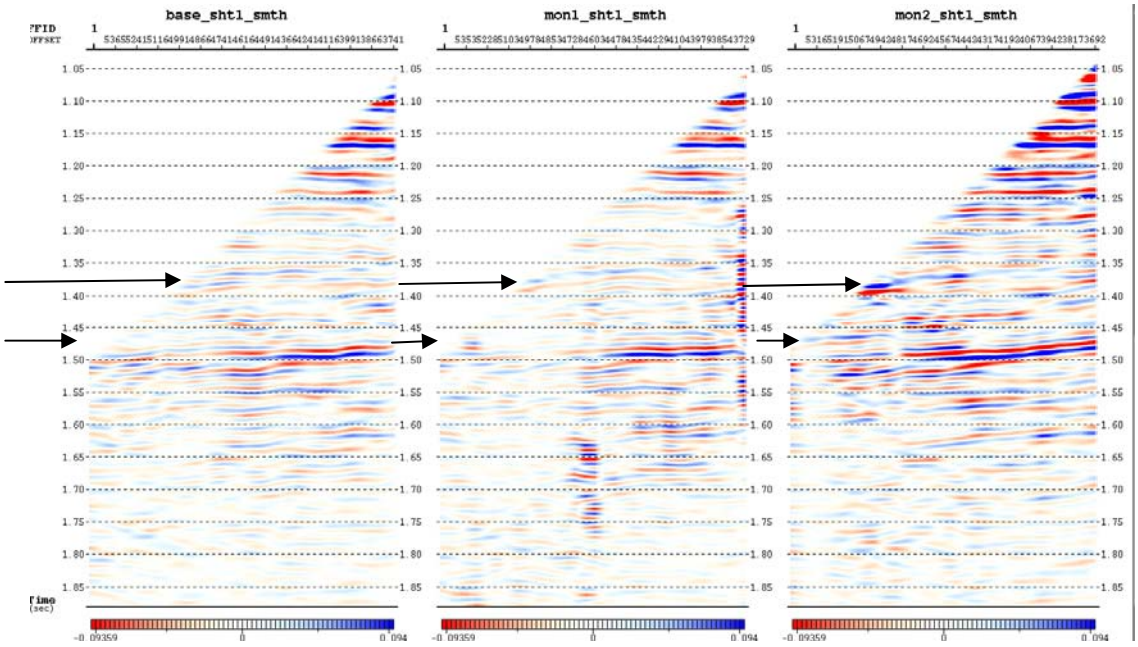

Figure 11: Base, monitor1, and Monitor2 for reservoirs Frio1 (arrows above) and Frio2 (arrows below)

The flow in Figure 10 has been run for each pair of data to calculate the subtracted section shown in Figure 12.

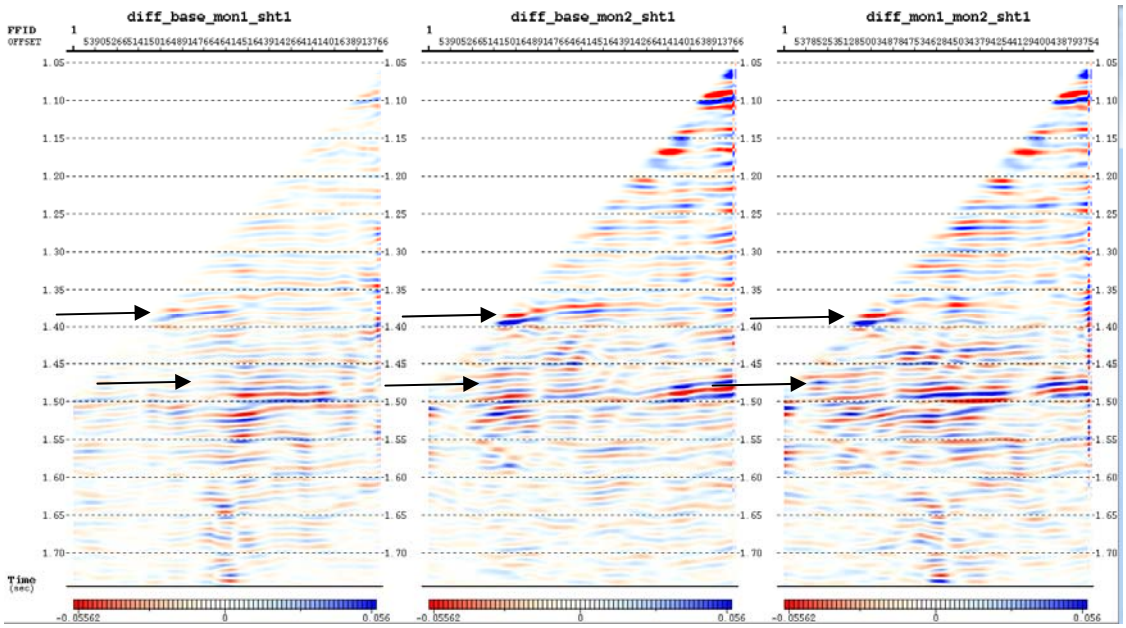

Figure 12: difference between each pair of data sets for base-monitor1, base-monitor2, and monitor1-monitor2 for site1.

6.2 NORMALIZED RMS (NRMS) AMPLITUDE CALCULATION

To evaluate the repeatability of seismic response after injection, a normalized root-mean-square criterion (Kragh and Christie, 2002) has been used. The RMS amplitude values have been calculated for all scenarios, base, monitor1, and monitor2, for specific windows of control reflectors as well as reservoir time interval windows. The formula for calculating NRMS is as follows:

$$NRMS = \frac{200 \times RMS(a_t - b_t)}{RMS(a_t) + RMS(b_t)}$$

where the RMS operator is defined as:

$$RMS(x_t) = \sqrt{\frac{\sum_{t_1}^{t_2} (x_t)^2}{N}}$$

where N is the number of samples in interval t1-t2.

By comparing the NRMS level of each pair of data sets (base-monitor1, base-monitor2, and monitor1-monitor2) we can estimate data repeatability. NRMS estimates can also show the possible effect of injected CO_2 underground, since the time-lapse change measured by NRMS can be due to reservoir changes. First we have used NRMS levels (plotted in percentage, with a range of 0-200) versus sensor depth, before and after preprocessing, to observe how a chosen preprocessing flow could enhance the time-lapse signal. We have begun with source site 1.

6.3 ANALYSIS OF CONTROL REFLECTION

Different control reflectors have been selected, time-shifted for alignment, and analyzed in terms of their NRMS level to find the best one in terms of minimizing NRMS level. The purpose of selecting the best control reflector is to remove the effect of overburden from the data so that we maximize the change in signal is due to the effect of injected CO_2. After time shifting to remove overburden variation, the repeatability of the control reflector can also be assessed with NRMS, and the reflector can be analyzed for amplitude normalization between each pair of surveys.

NRMS has been calculated in percentage versus sensor depth for several control reflector time windows, with three analyzed completely and two (1161-1168 ms, and 1355-1370 ms) described here. The NRMS response was used to choose the best control reflector among the three. Control reflector 2 was not effective in terms of improving the NRMS level of signal in the control reflector or the reservoir intervals. Control reflectors 1 and 3 have been studied and analyzed for NRMS responses after preprocessing.

6.4 CONTROL REFLECTOR 1

Figure 13 shows that there is not much improvement in NRMS using the first control reflector (1161-1168 ms) and analyzing the base-monitor1 pair. The effect of the median filter can be seen, but not an overall decrease in NRMS.

Figure 14 compares the improvement from control reflector 1 for the base-monitor2 pair, and we see that the average level of NRMS improved from 50% before preprocessing to 25% after preprocessing. Thus it shows 50% improvement in NRMS level. Figure 15 depicts the Monitor1-Monitor2 pair, and the average level of NRMS improved from 60% before preprocessing to 20% after preprocessing. In this case we do see a clear improvement in data repeatability with the preprocessing using control reflector 1.

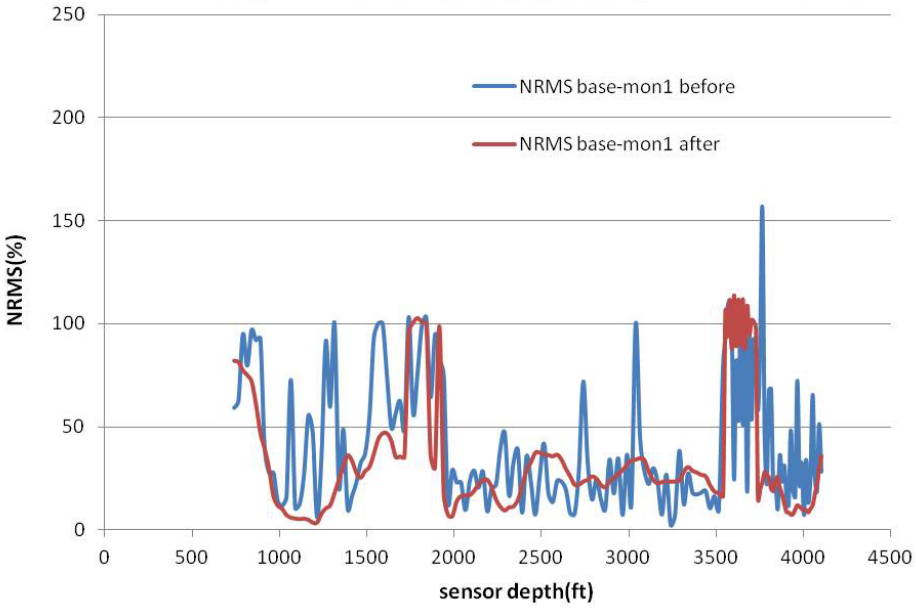

Figure 13: NRMS plot for before and after preprocessing, for base-monitor1 of first control reflector, 1161ms to 1168ms.

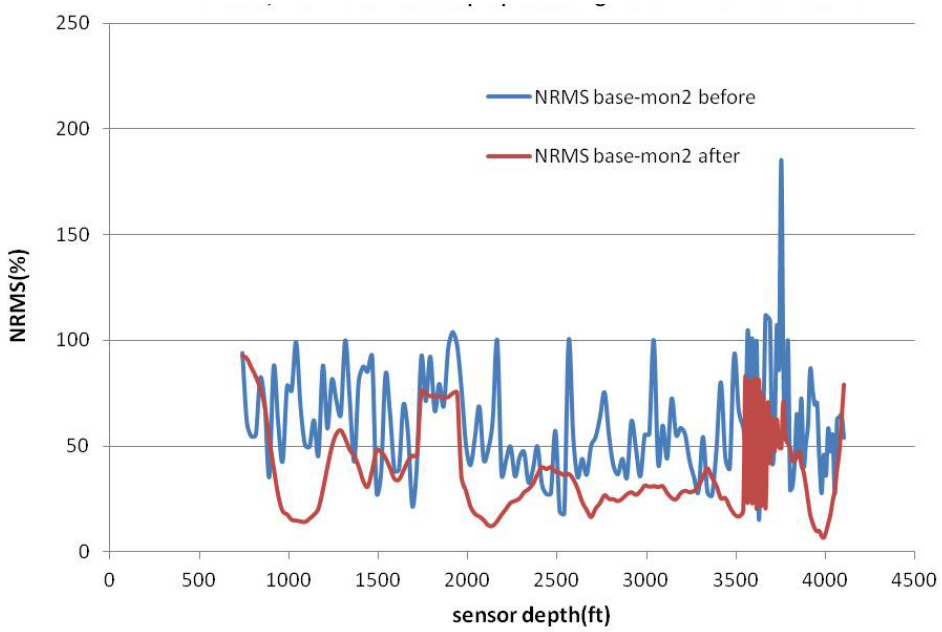

Figure 14: NRMS plot for before and after preprocessing, for base-monitor2 of first control reflector, 1161ms to 1168ms

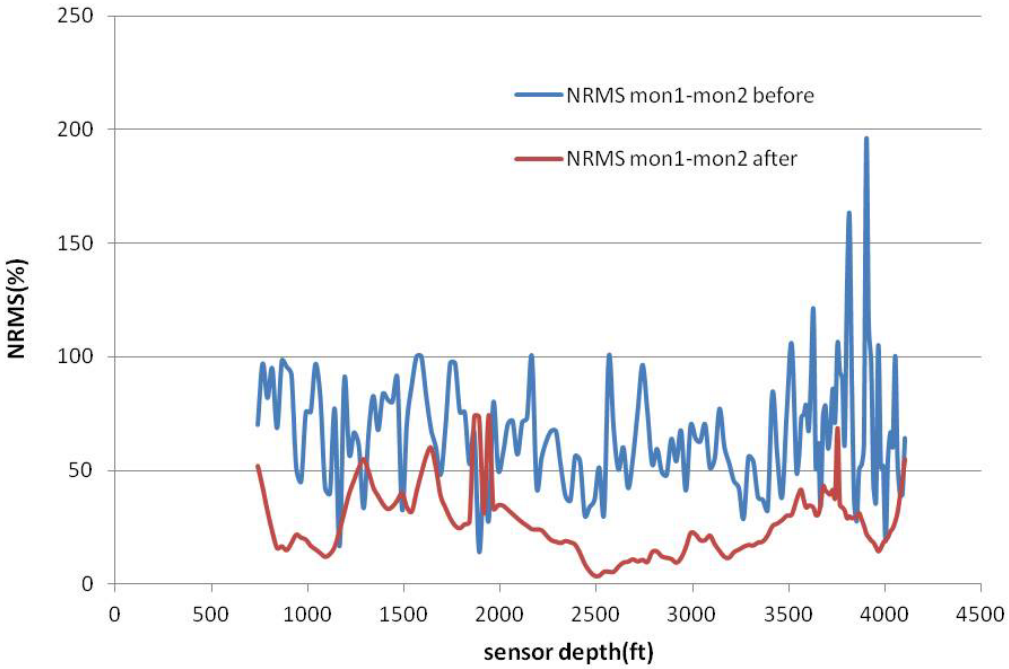

Figure 15: NRMS plot for before and after preprocessing, for monitor1-monitor2 of first control reflector, 1161ms to 1168ms

6.5 ANALYSIS OF RESERVOIR REFLECTION USING CONTROL 1

NRMS plots for reservoir intervals have been also analyzed versus sensor depths to see the effect of injection on Frio1 and Frio2 reservoirs. This analysis could also help to distinguish the effect of injected CO_2 plume into reservoir. The main focus in this part of the project is to interpret the NRMS response after preprocessing (red curves).

The effect of CO_2 plume in Frio1 reservoir should be observed in base-monitor1, and base-monitor2 scenarios, as the injection happens in Monitor1 stage and the effect of the CO_2 plume remains in the reservoir until Monitor2 occurs (assuming no migration of CO_2). Figure 16 shows the NRMS curve versus sensor depth for reservoir Frio1 interval (1380-1400 ms).

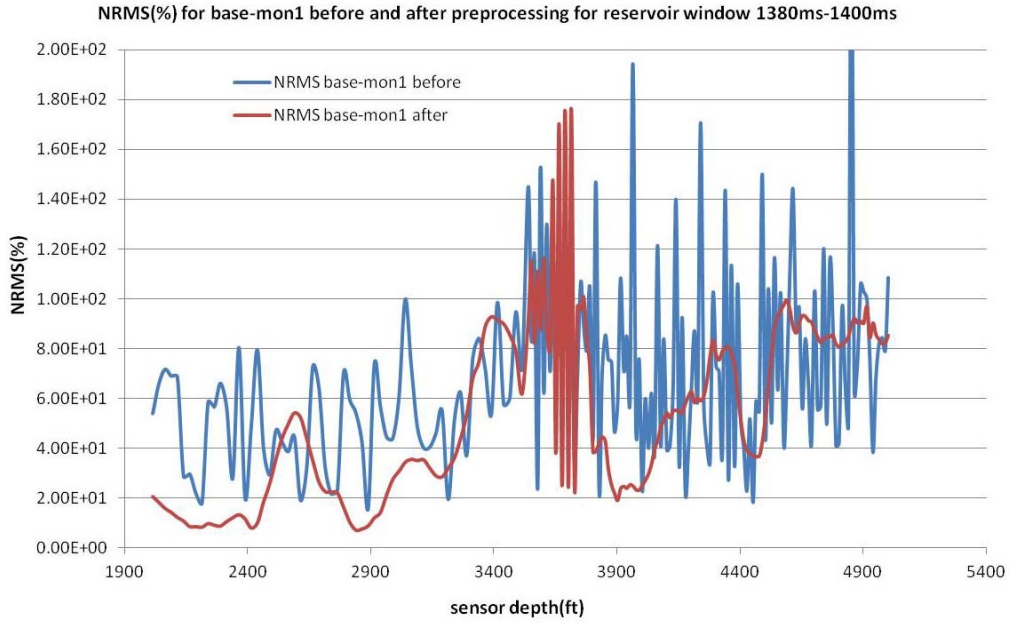

Figure 16: NRMS plot for before and after preprocessing, for base-monitor1 of first control reflector, for reservoir Frio1 1380ms to 1400ms

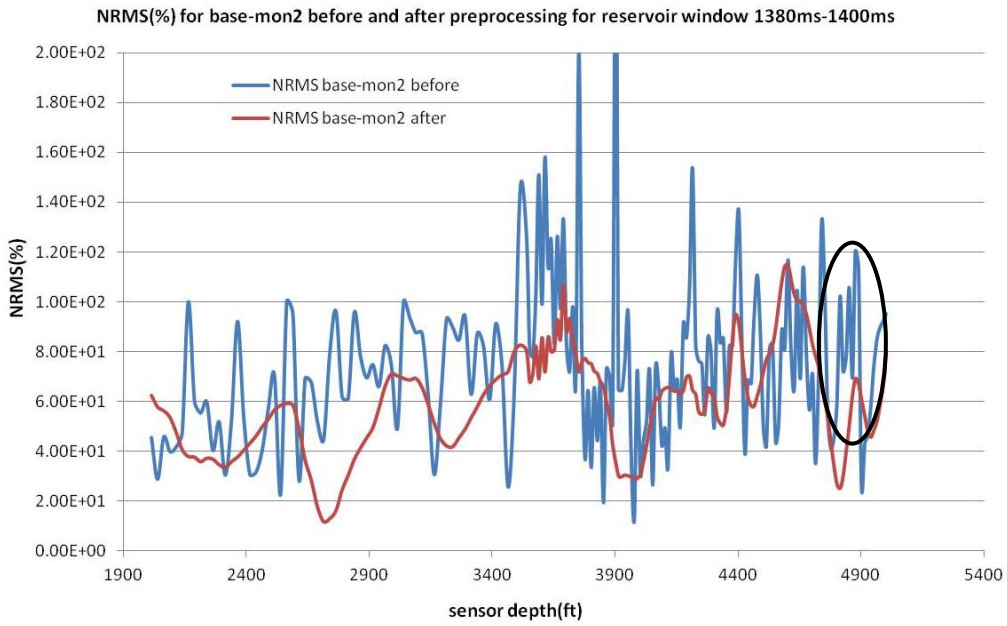

Figure 17: NRMS plot for before and after preprocessing, for base-monitor2 of first control reflector, for reservoir Frio1 1380ms to 1400ms

NRMS plots for reservoir intervals have been also been analyzed versus sensor depths to see the effect of injection on Frio1 and Frio2 reservoirs. Figure 17 shows the NRMS for base-monitor2 for the Frio1 reservoir zone. Figure 18 represents the NRMS level of reservoir Frio1, for the third scenario (monitor1-monitor2). It shows that the repeatability between these two surveys, monitor1 and monitor2 is improved by preprocessing. In Figures 16,17 and 18 there is no clear indication of increasing NRMS due to CO_2 injection.

The black circle on Figure 17 also shows where a time-lapse effect after CO_2 injection would be expected for reservoir Frio1 (sensor depth ~4900ft-5000ft). No clear indication is seen of NRMS rising above the background level (a rise that could be caused by the CO_2 injection).

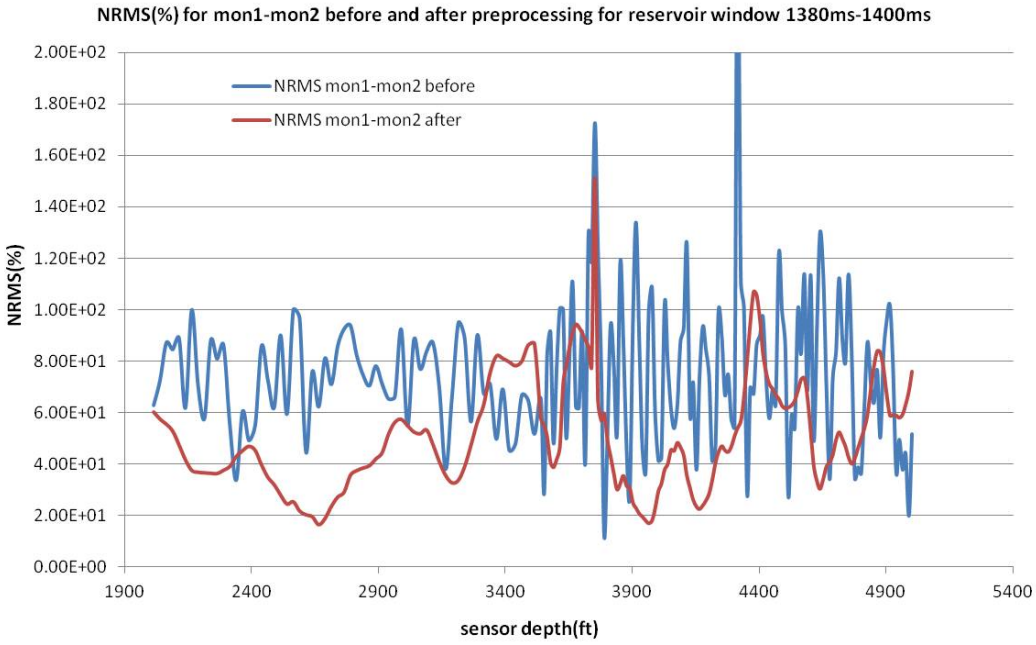

Figure 18: NRMS plot for before and after preprocessing, for monitor1-monitor2 of first control reflector, for reservoir Frio1 1380ms to 1400ms

For the Frio2 reservoir (~5400-5500 ft), Figure 19 shows that there is not much improvement in NRMS values from before to after preprocessing for the first scenario, base-monitor1. There is an increase in the circled zone, but it is not above the background level. For the second scenario, base-monitor2, in Figure 20, an improvement can be observed in NRMS level from 70% before preprocessing to 40% after preprocessing in reservoir Frio2. An increase in NRMS from 4500ft to 5000ft and also from 5300ft to 5400ft (near top reservoir Frio2) in Figure 20 shows the possible effect of CO_2 injection with NRMS rising to over 100% in the preprocessed data.

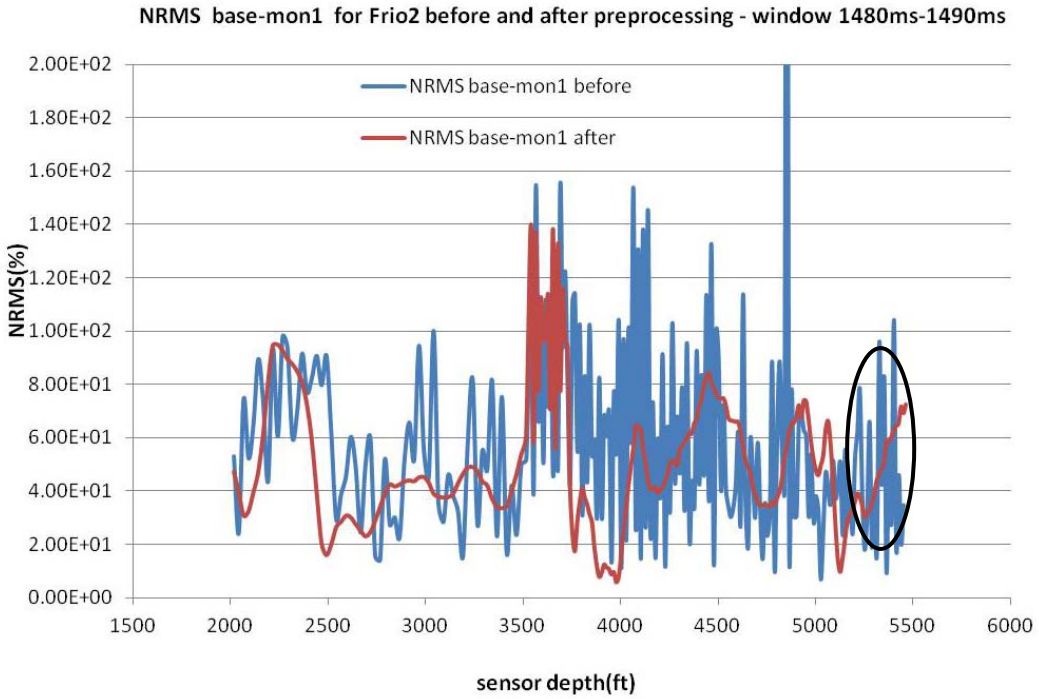

Figure 19: NRMS plot for before and after preprocessing, for base-monitor1 of first control reflector, for reservoir Frio2, 1480ms to 1490ms

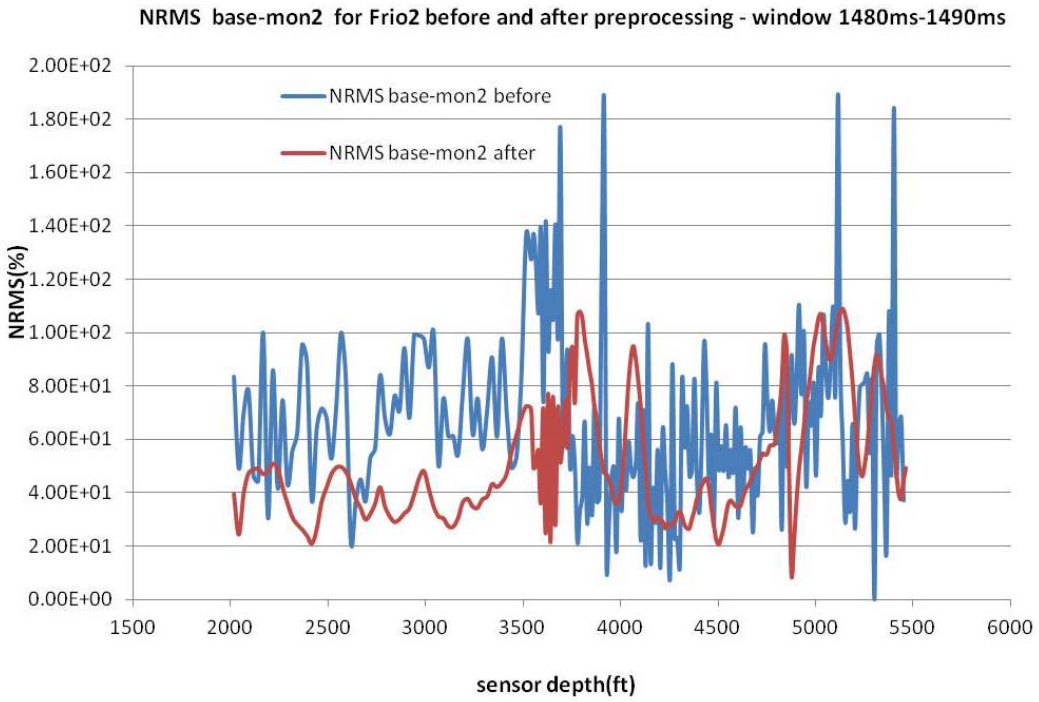

Figure 20: NRMS plot for before and after preprocessing, for base-monitor2 of first control reflector, for reservoir Frio2, 1480ms to 1490ms

Figure 21 represents the NRMS level for the third scenario, monitor1-monitor2. The injection in reservoir Frio2 occurred at monitor2 survey. The NRMS fluctuation observed at depth 2250ft cannot be due to CO_2 injection effect as it is repeated in both base-monitor1 and monitor1-monitor2 scenarios. An increase in NRMS level occurred at top reservoir Frio2 from 5000ft to 5300ft (large circle) could indicate the injection response.

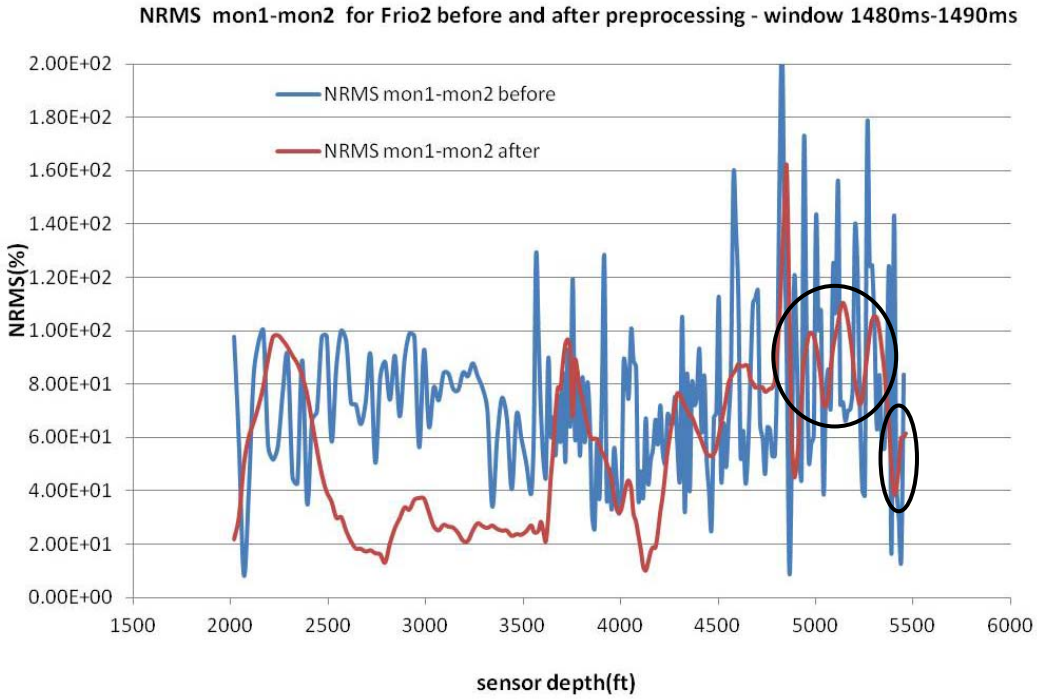

Figure 21: NRMS plot for before and after preprocessing, for monitor1-monitor2 of first control reflector, for reservoir Frio2, 1480ms to 1490ms

6.6 CONTROL REFLECTOR 3

Figure 22 and 23 show that using control reflector 3, the NRMS levels for before and after preprocessing steps have not been much improved for the first and second scenarios. Apparently, the first control reflector performs a better improvement on NRMS level for the first, base-monitor1, and second base-monitor2 scenarios. Although comparing scenario1 and scenario2, it appears that the average NRMS in second scenario slightly improved over 3100ft-4200ft sensor depths with 50% (from 80% to 40%) whereas there is not much improvement for the first scenario (Figure22) on the same depth range.

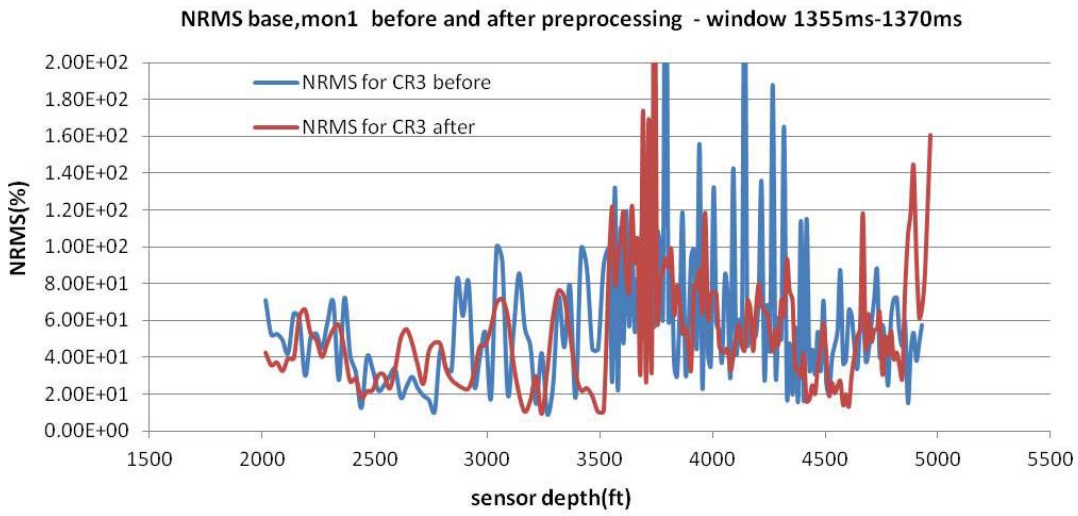

Figure 22: NRMS plot for before and after preprocessing, for base-monitor1 of third control reflector, 1355ms to 1370ms

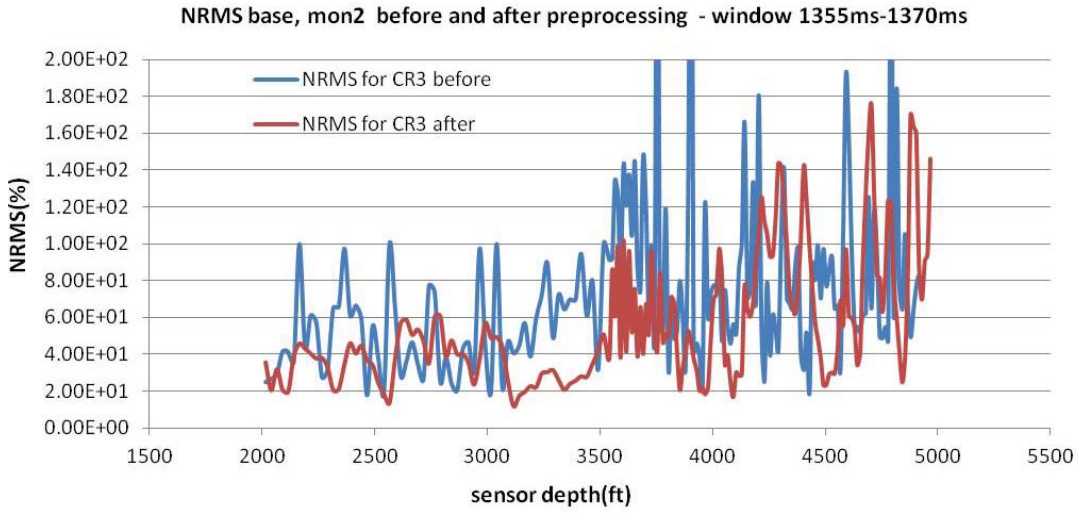

Figure 23: NRMS plot for before and after preprocessing, for base-monitor2 of third control reflector, 1355ms to 1370ms

Figure 24 shows the third scenario (mon1-mon2) with an average improvement of 30% in NRMS level from about 60% before preprocessing to 40% after. It is more promising than other two scenarios for control reflector 3 in terms of improvement in NRMS level.

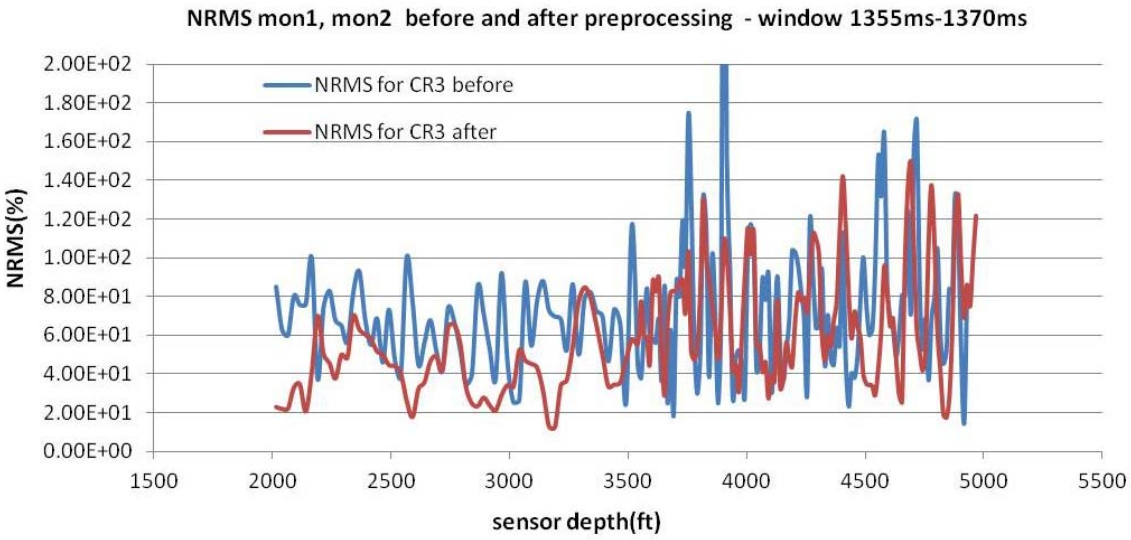

Figure 24: NRMS plot for before and after preprocessing, for monitor1-monitor2 of third control reflector, 1355ms to 1370ms

6.7 RESERVOIR FRIO1 REFLECTION USING CONTROL 3

Figure 25 depicts NRMS for Frio1 reservoir reflector (1380-1400 ms) using the third control reflector. An improvement in NRMS average level from 50% to 25% is seen for shallower sensors (2000ft-3500ft), but not for the deeper sensors where the CO_2 effect is expected (e.g. black circle in Figure). Comparing two control reflectors 1 and 3, we conclude that for the first scenario (base-monitor1) third control reflector has smaller NRMS values and for second (base-monitor2) and third (monitor1-monitor2) scenarios first control reflector shows a better response in terms of NRMS level

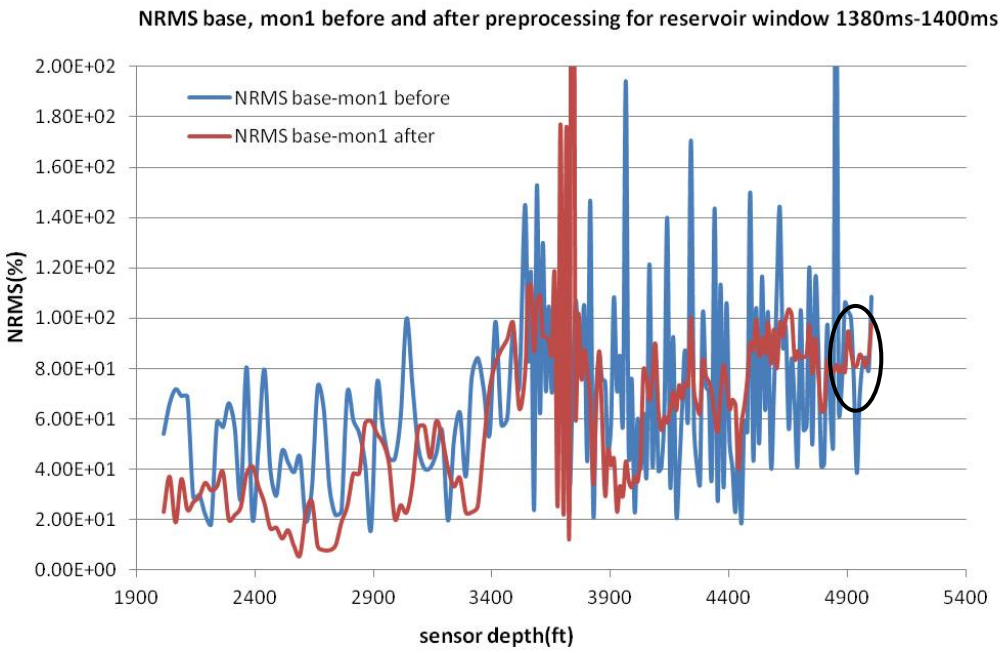

Figure 25: NRMS plot for before and after preprocessing, for base-monitor1 of third control reflector, for reservoir Frio1 1380ms to 1400ms

Figure 26 shows that the average NRMS level for the second scenario, base-monitor2 of reservoir Frio1, improved from about 60% to 40% after preprocessing. It also shows that the level of NRMS for reservoir Frio1 (4900ft-5000ft) remains low about 45% (black circle). Comparing Figure 25 and 26 at depth 4800ft-5000ft (reservoir Frio1), it is confirmed that there is comparable change in terms of NRMS values between base-monitor1 (80%) and base-monitor2 (60%) scenarios. Therefore the time-lapse response of CO_2 plume that could be seen in NRMS level for base-monitor1 scenario is possible, while in base-montiro2 scenario there is minimal change (no injection in monitor 2 survey in Frio1 reservoir).

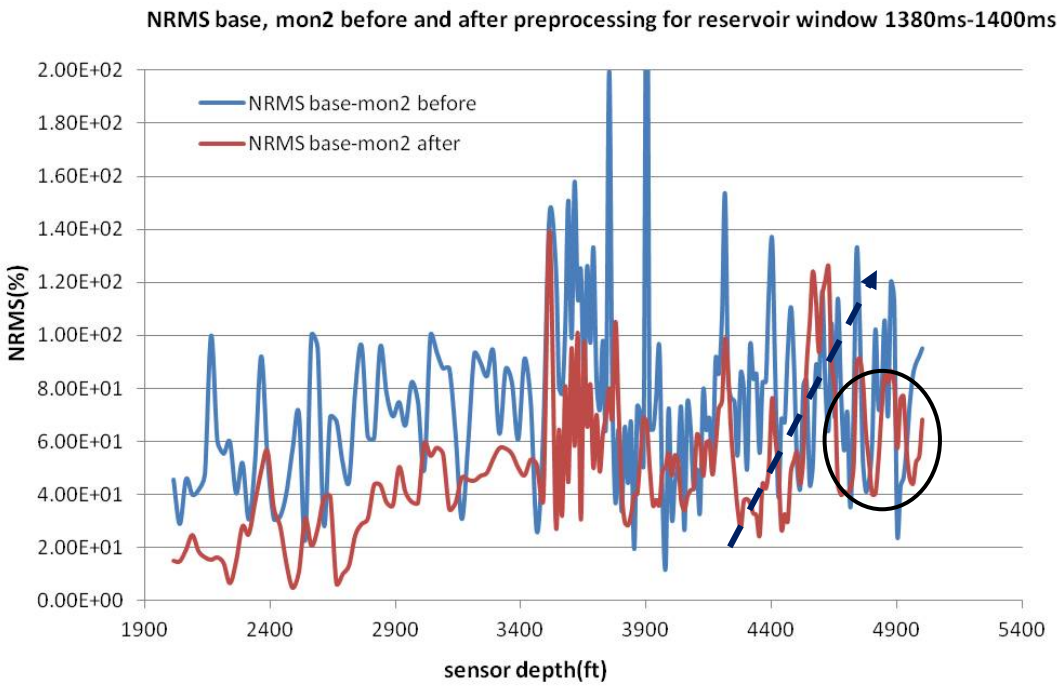

Figure 26: NRMS plot for before and after preprocessing, for base-monitor2 of third control reflector, for reservoir Frio1 1380ms to 1400ms

Figure 27 represents the NRMS curve for the third scenario, monitor1-monitor2 before and after preprocessing with control reflector 3 (1355-1370 ms). The NRMS level of reservoir Frio1 (sensor depth about 4900ft-5000ft) for third scenario (monitor1-monitor2) is 80% which is identical in compare with the second scenario. The first scenario and third are almost at the same NRMS level.

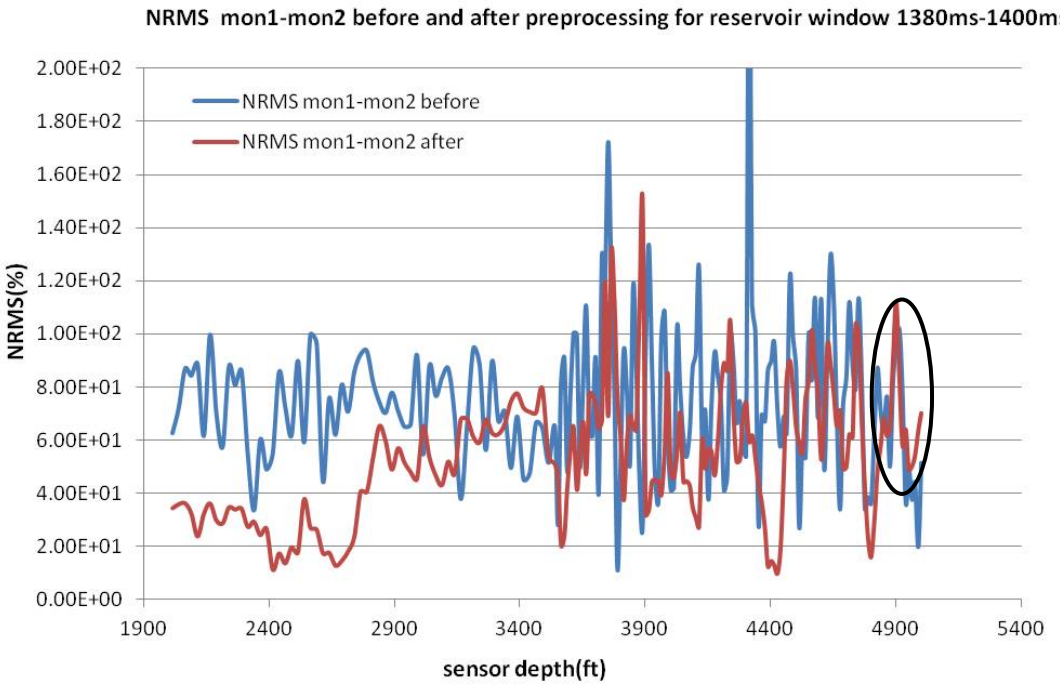

Figure 27: NRMS plot for before and after preprocessing, for monitor1-monitor2 of third control reflector, for reservoir Frio1 1380ms to 1400ms

6.8 RESERVOIR FRIO2 USING CONTROL REFLECTOR 3

Figure 28 shows the NRMS level for the Frio2 reservoir reflector (1480-1490 ms) for the base-monitor1 scenario. We see some improvement in NRMS over the 2000 – 2500 ft depth range, but not much improvement at the reservoir depths

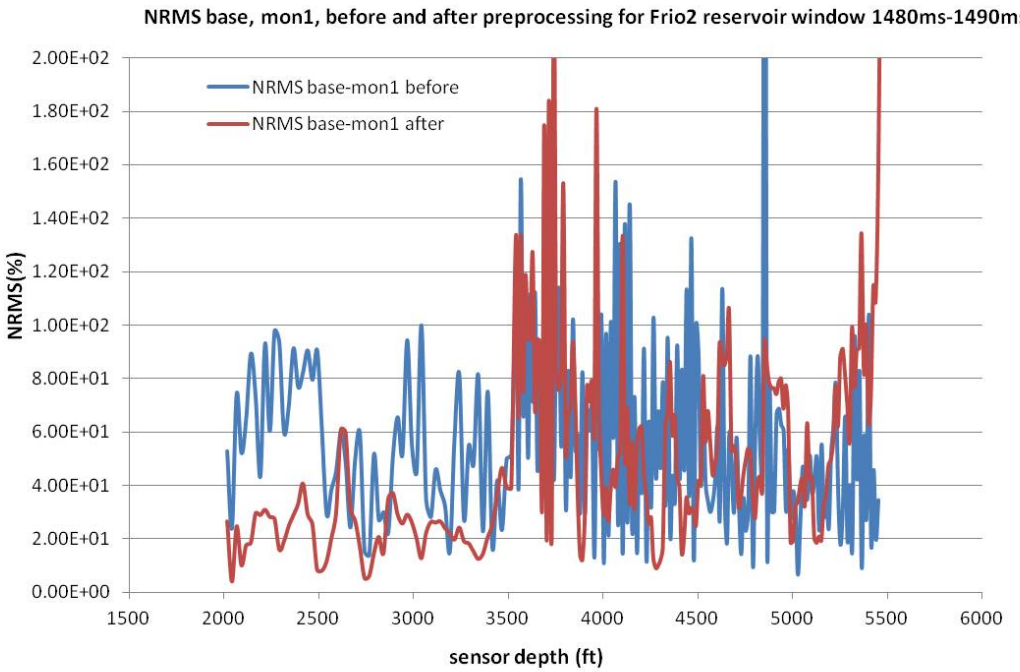

Figure 28: NRMS plot for before and after preprocessing, for base-monitor1 of third control reflector, for reservoir Frio2, 1480ms to 1490ms

Figure 29 shows the base-monitor2 scenario processed with control reflector 3 analyzed in the window of the Frio2 reservoir (1480-1490 ms). The effect of injected CO_2 in reservoir Frio2 (black circle) is not observable. Overall, the oscillation and increasing trend as shown by dashed arrow line in NRMS curve (green circle) indicates that the sensors above the reservoir had improvement in NRMS and NRMS level dramatically increased from 30%-40% to 80%-90% in average for sensors closer to top reservoir Frio1 (depth ~ 5000ft) and Frio2 (depth ~5400ft). This phenomenon could be seen in both Figures 29 and 30 below the sensor depth ~ 4300ft.

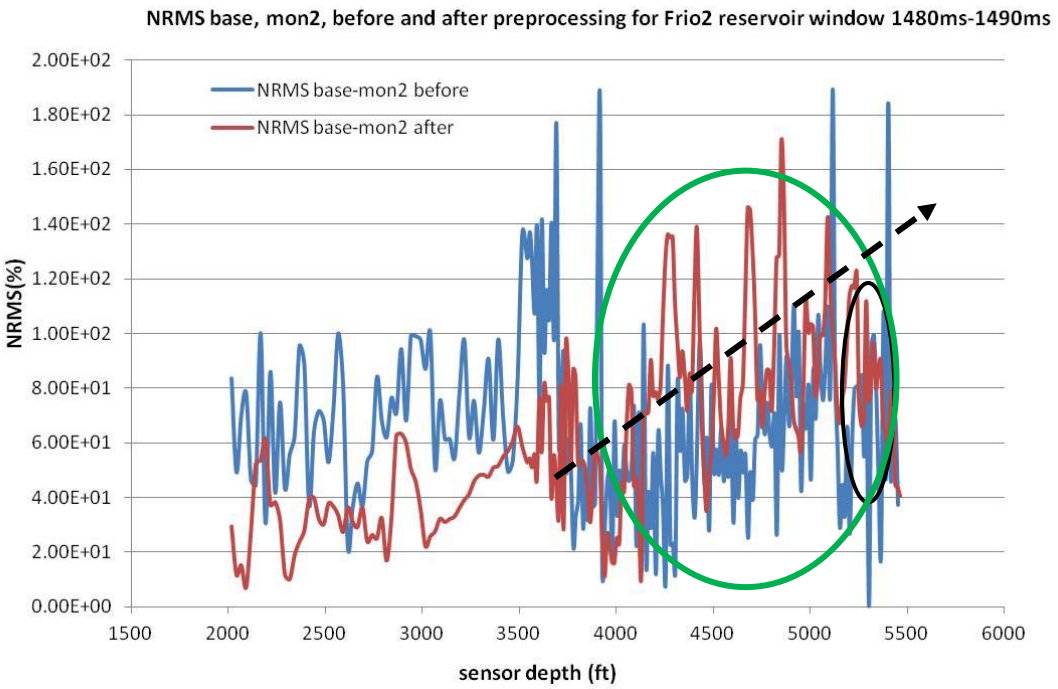

Figure 29: NRMS plot for before and after preprocessing, for base-monitor2 of third control reflector, for reservoir Frio2 1480ms to 1490ms

Figure 30, the NRMS for mon1-mon2 (scenario 3) represents that there is an increase in NRMS level for top reservoir Frio2 which has been shown by black circle, but it is not above the background variation.

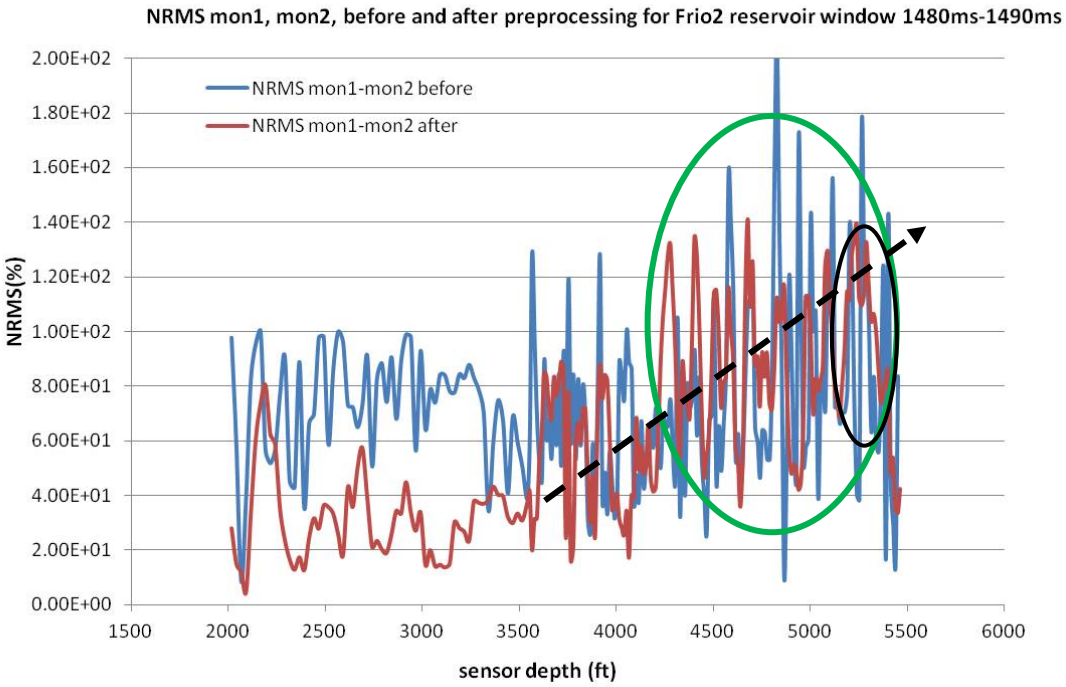

Figure 30: NRMS plot for before and after preprocessing, for monitor1-monitor2 of third control reflector, for reservoir Frio2 1480ms to 1490ms

6.9 AMPLITUDE CORRECTION

Like the static time shift applied in the above analysis, we expect the reflection amplitude to change due to temporal changes in the overburden. We attempt to remove this change by applying an amplitude correction based on analysis of the control reflector. Amplitude for all the seismic surveys has been corrected using a scaling factor. This factor has been calculated for all control reflector and reservoir windows. For all base, and monitor surveys, first control reflector window has been selected. Then the average RMS amplitude in that window (1100ms-1280ms) has been calculated. Finally all the sample amplitude values of the data set are divided by that average RMS value. This amplitude correction procedure has been applied to data from site 1 and site 4. The correction (inverse of average RMS amplitude values) for site 1 for base, monitor1, and monitor2, are 13.20, 12.01, and 8.74, respectively. For site4, the values for base, monitor1, and monitor2 are 15.36, 18.11, and 11.94, respectively.

Figure 31 shows the NRMS level after amplitude correction for the first scenario, base-monitor1 for site 1. The entire section has been corrected using a scale factor calculated in the 1100ms to 1280ms window for the first control reflector. It seems that the level of NRMS after correction has been slightly increased.

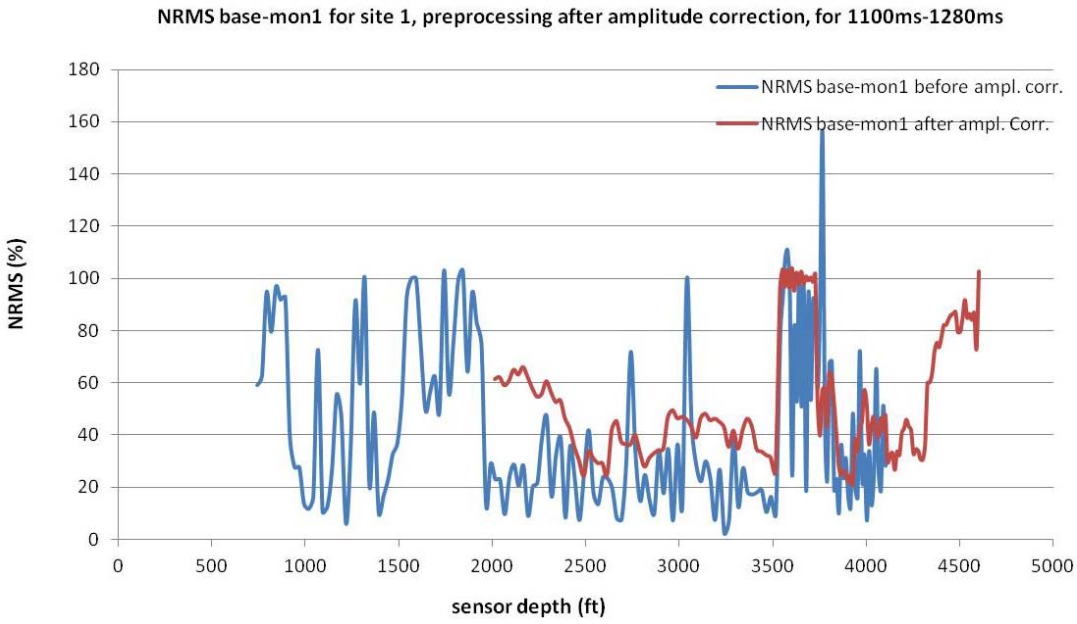

Figure 31: NRMS plot for before and after preprocessing, for base-monitor1 of first control reflector, after amplitude correction.

Figure 32 also shows the level of NRMS for the second scenario, base-monitor2, after amplitude correction. It depicts that the NRMS level has been slightly improved (decreased) over 3000ft-4200ft of sensor depth.

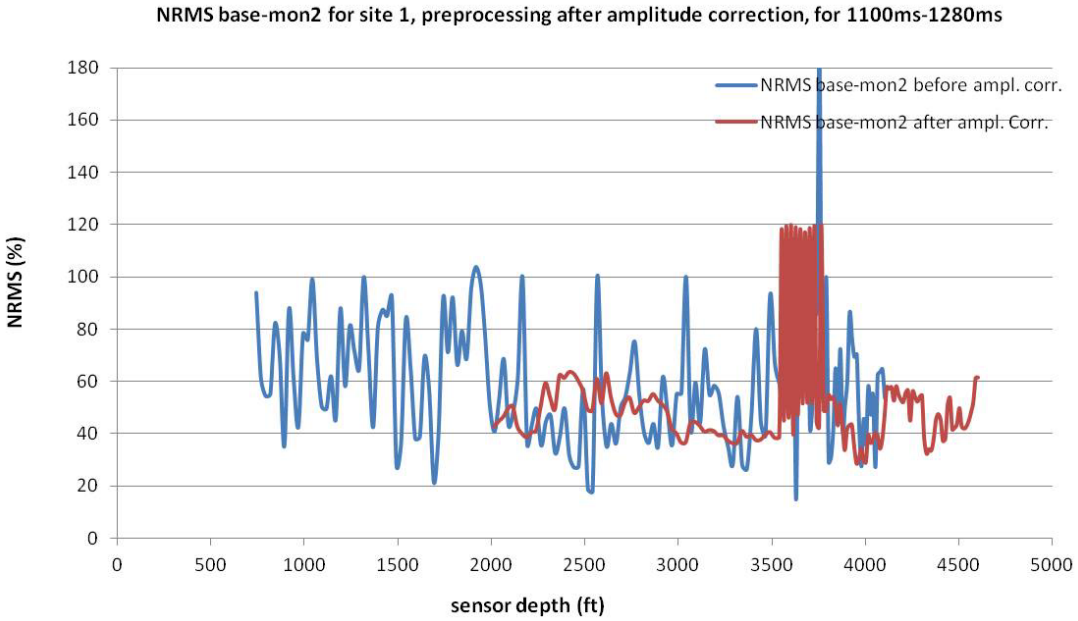

Figure 32: NRMS plot for before and after preprocessing, for base-monitor2 of first control reflector, after amplitude correction.

Figure 33 represents the level of NRMS amplitude for the third scenario, monitor1-monitor2, after amplitude correction. It depicts that the NRMS level has been improved over 2500ft-4500ft of sensor depth.

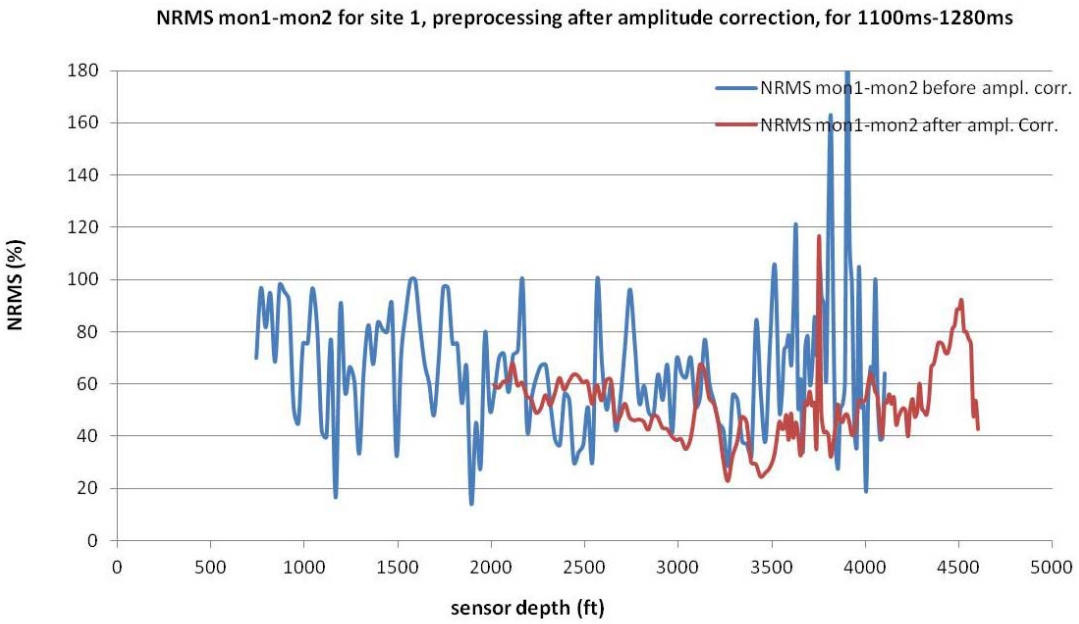

Figure 33: NRMS plot for before and after preprocessing, for monitor1-monitor2 of first control reflector, after amplitude correction

7. ANALYSIS AND DISCUSSION

A data set regarding the construction of wells in the vicinity of the hypothetical Kimberlina CO_2 injection was assembled from public records and analyzed. Approximately 100 wells encountered the Vedder Formation storage target within the region with a simulated 6 bar pressure increase at the end of injection. Visualization of the well's construction indicated a large proportion of the borings contained cement over a relatively short fraction of their length both within the simulated CO_2 plume area as well as the surrounding area of elevated pressure. Summarizing the analysis we use the processed (time-shift and amplitude correction) data to compare NRMS values for the two reservoir reflectors, first using control reflector 1 for the three scenarios: base-mon1 (Figure 34), base-mon2 (Figure 35), mon1-mon2 (Figure 36), and then using control reflector 3 for the three scenarios: base-mon1 (Figure 37), base-mon2 (Figure 38), mon1-mon2 (Figure 39). In Figure 34 we compare the first control reflector, the Frio1 and Frio2 reflectors and see NRMS level for both reservoirs Frio1 and Frio2 to be above the first control reflector. Higher level of NRMS in these two reservoirs compared with control reflector could be either due to higher level of noise or the effect of injected CO_2 gas. NRMS values of 80% for reservoir Frio1, (seen when normalizing by both first and third control reflectors), indicates that the injection at reservoir Frio1 may be detected (black circle in Figure 34). On the other hand the NRMS trend for reservoir Frio2 remains stable as expected since no injection occurred in Frio2 between base and mon1. Some changes in Frio2 curve (in both Figures 34 and 37) could be possibly due to the effect of CO_2 gas injection into reservoir Frio1 located above the reservoir Frio2. However the overall high NRMS values and data variability limit interpretation quality.

For reservoir Frio2 and in specific the second and third scenarios for that reservoir, one could observe that there is an increasing trend in NRMS with depth as shown in Figure 35 for sensors immediately above the reservoir (circle in Figures 35 and 36). This is a possible indicator that CO_2 gas injection occurred in that reservoir. This trend could also be observed in Figures 38 and 39.

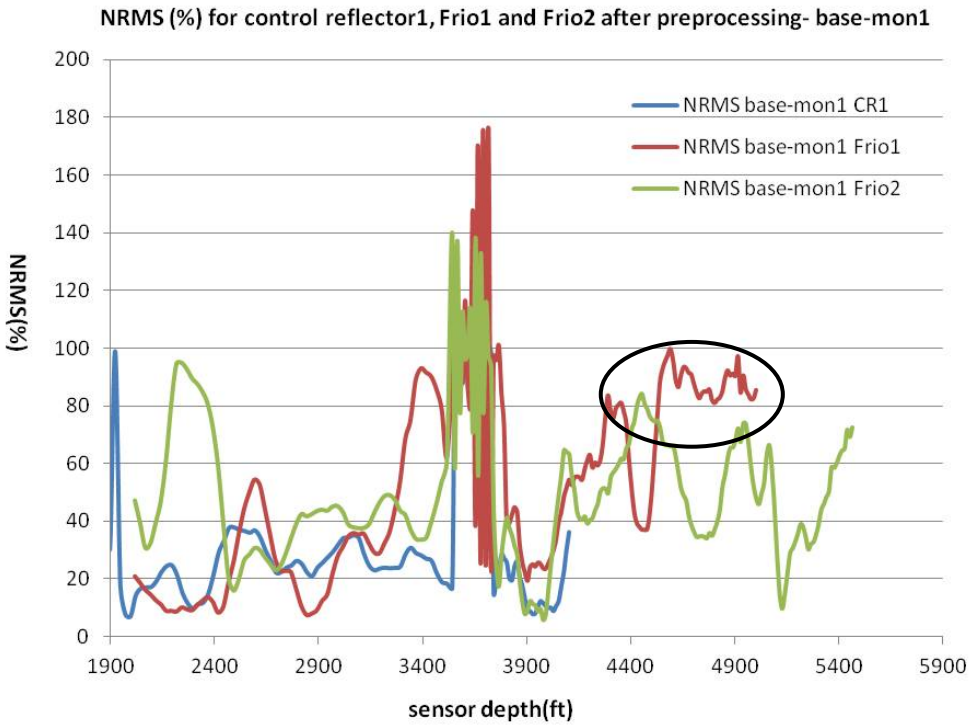

Figure 34: NRMS plot for before and after preprocessing, for Base-monitor1 scenario of Control reflector1, reservoirs Frio1 and Frio2

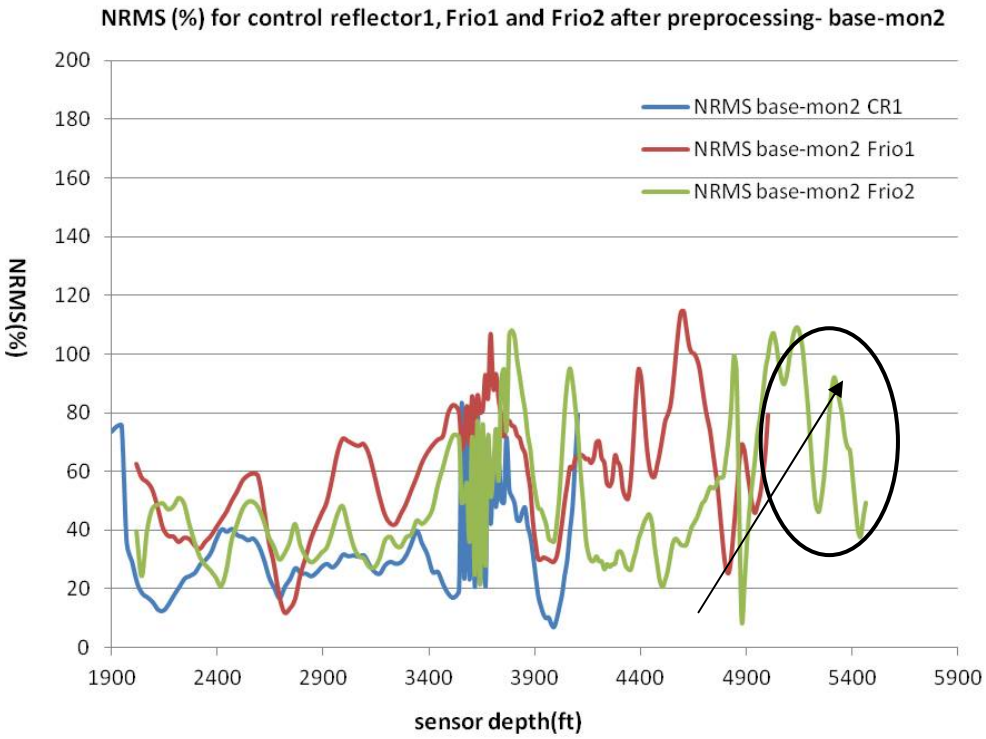

Figure 35: NRMS plot for before and after preprocessing, for Base-monitor2 scenario of Control reflector1, reservoirs Frio1 and Frio2

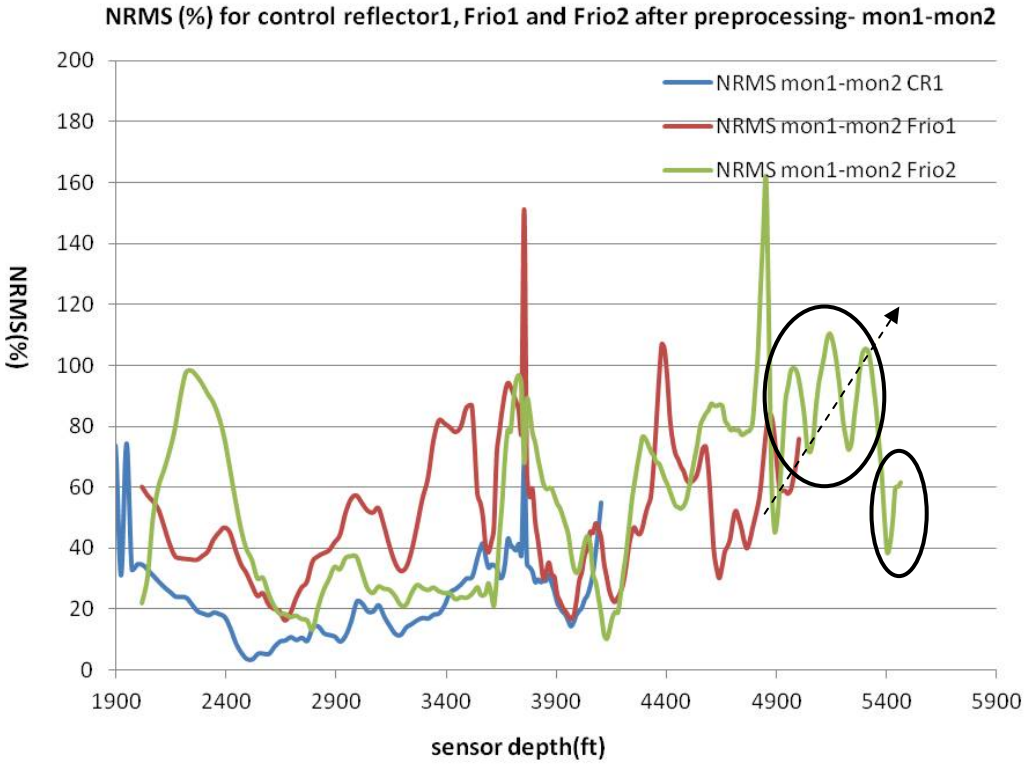

Figure 36: NRMS plot for before and after preprocessing, for monitor1-monitor2 scenario of Control reflector1, reservoirs Frio1 and Frio2

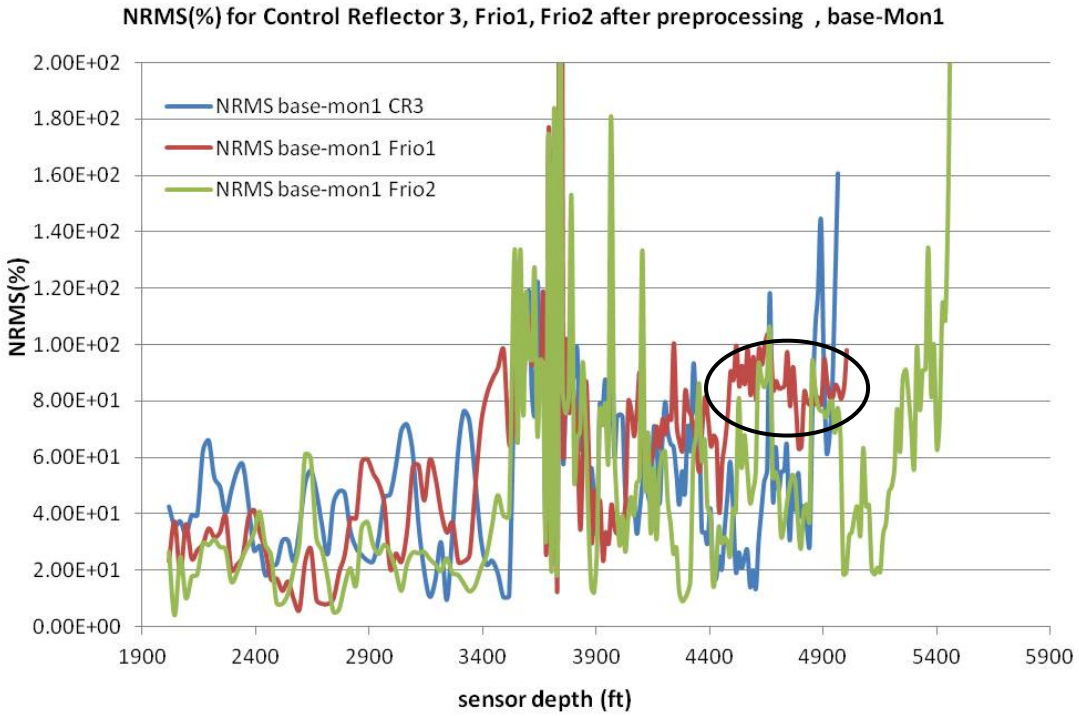

Figure 37: NRMS plot for before and after preprocessing, for base-monitor1 scenario of Control reflector3, reservoirs Frio1 and Frio2

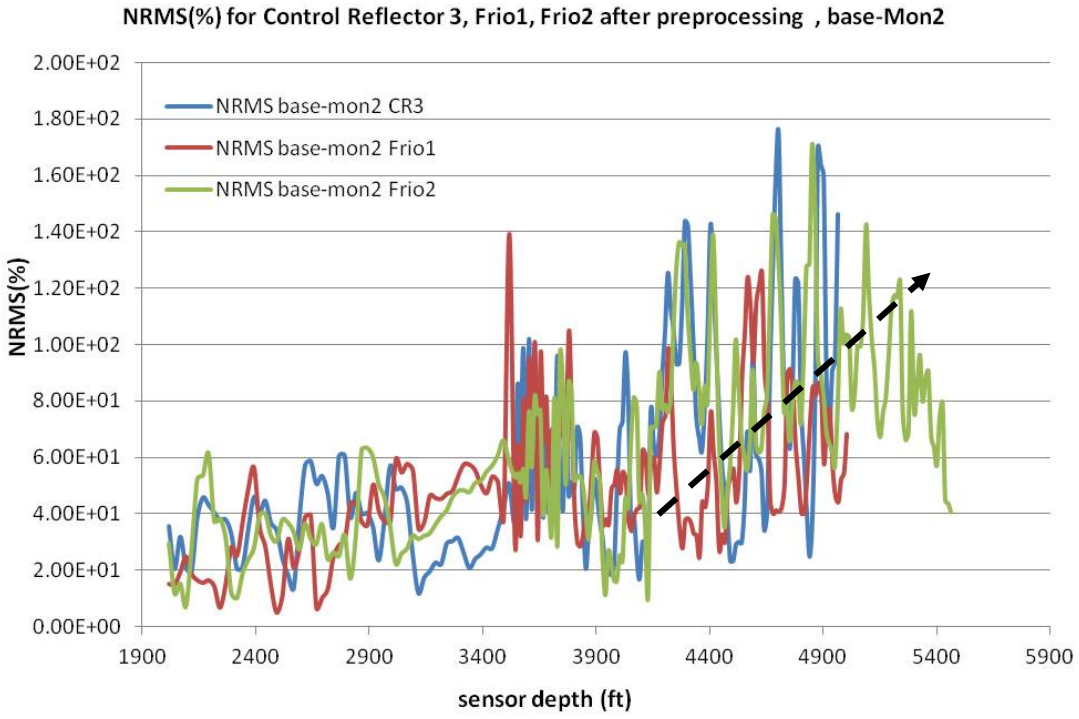

Figure 38: NRMS plot for before and after preprocessing, for base-monitor2 scenario of Control reflector3, reservoirs Frio1 and Frio2

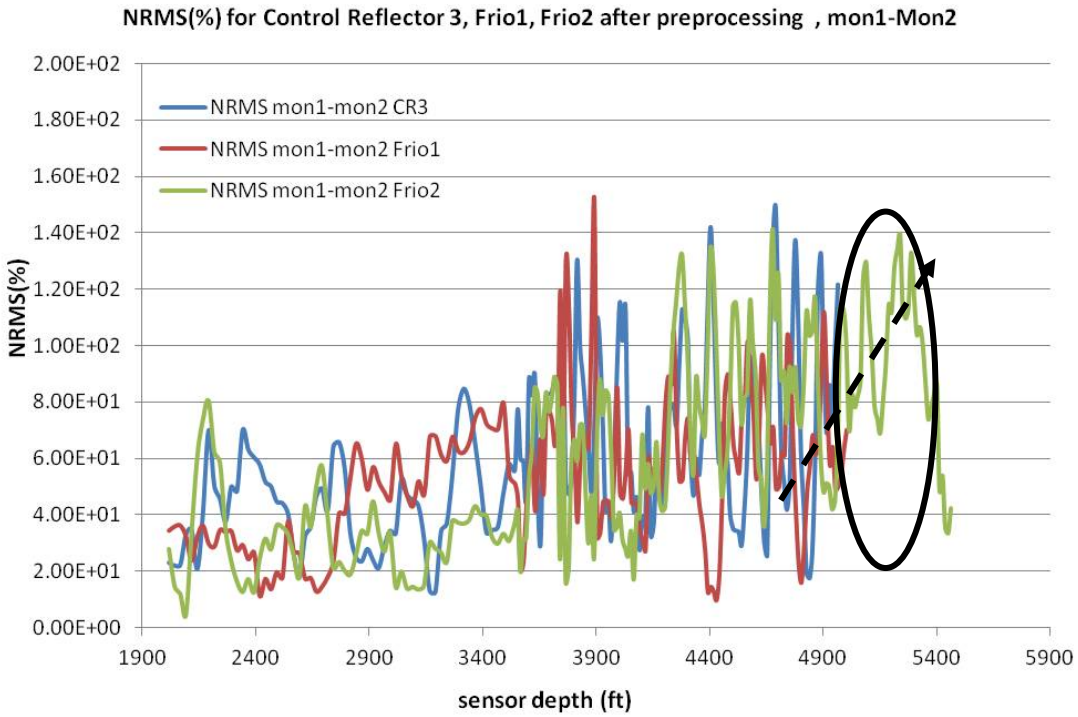

Figure 39: NRMS plot for before and after preprocessing, for monitor1-monitor2 scenario of Control reflector3, reservoirs Frio1 and Frio2

8. CONCLUSIONS

The use of NRMS to quantify detectability in time-lapse VSP data was tested on the Frio Pilot data. Basic processing of static time-shifts and amplitude corrections, calculated on a control reflector did prove useful in reducing the time-lapse noise. The overall data repeatability was in the range of 30-80% NRMS. This relatively high level of time-lapse noise limited the interpretation of the data. Suggestions of detectable changes via NRMS values could be found in the Frio data where the NRMS values increased for deeper sensors which correspond to reflection points near the injection well where CO_2 saturation is expected to be high.

The NRMS calculation was shown to be a useful measure of a given processing algorithm's ability to reduce time-lapse noise. Uncertainty in CO_2 detection remains high following the basic processing applied here. While changes in reflections at the injection level could be detected, they remain approximately equal to the time-lapse noise in the entire data set, as measured by NRMS. The overall NRMS for the Frio VSP, in the range of 30% to 80%, following basic processing, could be considered as an estimated baseline in assessing the utility of VSP for CO_2 monitoring. However, we do expect that further processing has the potential to reduce the estimated NRMS values for this data set.

9. REFERENCES

Daley, T.M., Myer, L.R., Peterson, J.E., Majer, E.L., Hoversten, G.M., 2008, Time-lapse crosswell seismic and VSP monitoring of injected CO_2 in a brine aquifer, Environmental Geology, 54, 1657-1665, DOI:10.1007/s00254-007-0943-z.

Daley, Thomas M., Jonathan B. Ajo-Franklin, Christine Doughty, 2011, Constraining the reservoir model of an injected CO_2 plume with crosswell CASSM at the Frio-II brine pilot, International Journal of Greenhouse Gas Control, 5, pp. 1022-1030, DOI information: 10.1016/j.ijggc.2011.03.002.

Daley, T.M. and Hovorka, S. D., 2010, Site closure monitoring of two CO_2 plumes with VSP at the Frio Pilot, American Geophysical Union Fall Meeting, H13C-0983, Dec. 2010, San Francisco, California.

Hardage, B. A., 2000, Vertical seismic profiling: principles: third updated and revised edition: New York, Pergamon, Seismic Exploration, v. 14, 552 p.

Hovorka, S.D., Benson. S.M., Doughty, C., Freifeld, B.M., Sakurai, S., Daley, T.M., Kharaka, Y.K, Holtz, M.H., Tarutz, R.C., Nance, S.H., Myer, L.R. and Knauss K.G., 2006, Measuring permanence of CO_2 storage in saline formations: the Frio experiment, Environmental Geosciences, V. 13, no 2, pp 1-17, DOI:10.1306/eg.11210505011.

Kragh, E., and Christie, P., 2002, Seismic repeatability, normalized rms, and predictability, The Leading Edge Jul 2002, Vol. 21, No. 7, pp. 640-647

Lumley, D. et al., 4D seismic risk analysis spreadsheet, SEG abstract, 1997, 2000.

SR2020, 2009, VSP Processing, Presentation report, July 14, 2009.

Zhou, Rongmao, Lianjie Huang, James T. Rutledge, Michael Fehler, Thomas M. Daley, Ernest L. Majer, 2010, Coda-wave interferometry analysis of time-lapse VSP data for monitoring geological carbon sequestration, International Journal of Greenhouse Gas Control, 4, 679–686, doi:10.1016/j.ijggc.2010.01.010. LBNL-3076E.

nrap
National Risk
Assessment Partnership

NRAP is an initiative within DOE's Office of Fossil Energy and is led by the National Energy Technology Laboratory (NETL). It is a multi-national-lab effort that leverages broad technical capabilities across the DOE complex to develop an integrated science base that can be applied to risk assessment for long-term storage of carbon dioxide (CO_2). NRAP involves five DOE national laboratories: NETL-RUA, Lawrence Berkeley National Laboratory (LBNL), Lawrence Livermore National Laboratory (LLNL), Los Alamos National Laboratory (LANL), and Pacific Northwest National Laboratory (PNNL). The NETL-RUA is an applied research collaboration that combines NETL's energy research expertise in the Office of Research and Development (ORD) with the broad capabilities of five nationally recognized, regional universities—Carnegie Mellon University (CMU), The Pennsylvania State University (PSU), the University of Pittsburgh (Pitt), Virginia Tech (VT), and West Virginia University (WVU)—and the engineering and construction expertise of an industry partner (URS Corporation).

NRAP Technical Leadership Team

Jens Birkholzer
LBNL Technical Coordinator
Lawrence Berkeley National Laboratory
Berkeley, CA

Grant Bromhal
NETL Technical Coordinator
Lead, Reservoir Working Group
Office of Research and Development
National Energy Technology Laboratory
Morgantown, WV

Chris Brown
PNNL Technical Coordinator
Lead, Groundwater Working Group
Pacific Northwest National Laboratory
Richmond, WA

Susan Carroll
LLNL Technical Coordinator
Lawrence Livermore National Laboratory
Livermore, CA

Laura Chiaramonte
Lead, Natural Seals Working Group
Lawrence Livermore National Laboratory
Livermore, CA

Tom Daley
Lead, Monitoring Working Group
Lawrence Berkeley National Laboratory
Berkeley, CA

George Guthrie
Technical Director, NRAP
Office of Research and Development
National Energy Technology Laboratory
Pittsburgh, PA

Rajesh Pawar
LANL Technical Coordinator
Lead, Systems Modeling Working Group
Los Alamos National Laboratory
Los Alamos, NM

Tom Richard
Deputy Technical Director, NRAP
The Pennsylvania State University
NETL-Regional University Alliance
State College, PA

Brian Strazisar
Lead, Wellbore Integrity Working Group
Office of Research and Development
National Energy Technology Laboratory
Pittsburgh, PA

nrap
National Risk
Assessment Partnership

Sean Plasynski
Deputy Director
Strategic Center for Coal
National Energy Technology Laboratory
U.S. Department of Energy

Jared Ciferno
Director
Office of Coal and Power R&D
National Energy Technology Laboratory
U.S. Department of Energy

Robert Romanosky
Technology Manager
Office of Coal and Power R&D
National Energy Technology Laboratory
U.S. Department of Energy

Regis Conrad
Director
Division of Cross-cutting Research
Office of Fossil Energy
U.S. Department of Energy

NRAP Executive Committee

Cynthia Powell
Director
Office of Research and Development
National Energy Technology Laboratory
U.S. Department of Energy

Alain Bonneville
Laboratory Fellow
Pacific Northwest National Laboratory

Donald DePaolo
Associate Laboratory Director
Energy and Environmental Sciences
Lawrence Berkeley National Laboratory

Melissa Fox
Chair, NRAP Executive Committee
Program Manager
Applied Energy Programs
Los Alamos National Laboratory

Julio Friedman
Chief Energy Technologist
Lawrence Livermore National
Laboratory

George Guthrie
Technical Director, NRAP
Office of Research and Development
National Energy Technology Laboratory

NRAP Technical Report Series